J Gastroenterol 2008; 43:589–596
DOI 10.1007/s00535-008-2198-1

Journal of Gastroenterology

Endoscopic characterization of the small bowel in patients with portal hypertension evaluated by double balloon endoscopy

Mayumi Kodama[1,2], Hirofumi Uto[3], Masatsugu Numata[4], Takeshi Hori[1], Takanobu Murayama[1], Fumisato Sasaki[3], Naoko Tsubouchi[3], Akio Ido[3], Kazuya Shimoda[2], and Hirohito Tsubouchi[3,4]

[1]Miyazaki Medical Center Hospital, Center for Digestive and Liver Diseases, Miyazaki, Japan
[2]Department of Gastroenterology and Hematology, Faculty of Medicine, University of Miyazaki, Miyazaki, Japan
[3]Department of Digestive and Life-style Related Disease, Kagoshima University Graduate School of Medical and Dental Sciences, 8-35-1 Sakuragaoka, Kagoshima 890-8520, Japan
[4]Department of Experimental Therapeutics, Translational Research Center, Kyoto University Hospital, Kyoto, Japan

Background. The endoscopic abnormalities present in the small bowel (SB) of patients with portal hypertension (PH) are not well understood. This study sought to evaluate endoscopic findings of the SB in patients with PH by double balloon endoscopy (DBE). ***Methods.*** We evaluated the endoscopic findings of SB in 15 patients with PH and 49 controls without liver disease or PH. A total of 24 and 90 procedures were performed for PH patients and control patients, respectively, through oral and/or anal approaches. ***Results.*** Fourteen of the 15 patients exhibited villous abnormalities, including edema (73%), atrophy (40%), and reddening (47%) of villi. Vascular lesions, such as angiodysplasia-like abnormalities (67%), dilated/proliferated vessels (93%), and varices (7%), were observed in all patients with PH. Although they were associated with ascites, these abnormalities did not correlate with any laboratory findings. None of these abnormalities was observed in controls. Definitive or suspected bleeding sources were identified in 9 of 13 patients with both PH and obscure gastrointestinal bleeding (OGIB), which was similar to the incidence in controls with OGIB. Although the frequency of postprocedure fever (>37.5°C) was higher in patients with PH in comparison to controls (29% vs. 2%, $P < 0.01$), endoscopic treatment under DBE was performed on 3 PH patients without serious complications. ***Conclusions.*** Endoscopic abnormalities of the SB may be prevalent in patients with PH. Although postprocedure fever of DBE may occur more commonly in patients with PH, DBE is useful as both a diagnostic and therapeutic tool to evaluate the SB.

Key words: portal hypertensive enteropathy, double balloon endoscopy, portal hypertension, liver cirrhosis, small bowel

Received: November 26, 2007 / Accepted: March 30, 2008
Reprint requests to: H. Uto

Introduction

Portal hypertension (PH) can be caused by hepatic fibrosis or obstruction of the portal vein. Hepatic fibrosis, of which liver cirrhosis is an advanced form, results from chronic liver disease. PH has numerous complications bearing high morbidity and mortality, including variceal bleeding. Splanchnic blood flow is significantly altered by PH.[1,2] Varices develop in the esophagus, stomach, duodenum, colon, or rectum. Portal hypertensive gastropathy (PHG) or colopathy follow the development of PH and can lead to gastrointestinal bleeding. There is a subset of cases, however, in which the bleeding source remains unclear following upper and lower gastrointestinal endoscopies in patients with PH.[3–6]

The changes in the gastrointestinal mucosa of the esophagus, stomach, colon, and rectum are well described in patients with PH. The majority of studies have focused on the involvement of the gastric and colonic mucosa in patients with PH; however, it is likely that the small bowel (SB), including the duodenum and ileum, would also undergo mucosal changes as a result of PH, which is defined as portal hypertensive enteropathy (PHE).[7,8] As the SB is distal to both the mouth and the anus, it is difficult to evaluate the entire SB by endoscopic diagnosis using upper and lower gastrointestinal endoscopy; regions of the small intestine will always lie beyond the limits of the endoscope. Therefore, the endoscopic abnormalities in the SB of patients with PH have not been well characterized.

Recently, new endoscopic methods, video capsule endoscopy (VCE) and double balloon endoscopy (DBE), have been developed for examination of the entire SB.[9,10] VCE permits direct visualization of the SB mucosa. Although VCE is both easy and painless, this technique usually does not allow visualization in real time. In addition, the technology is limited by the inability to take biopsies for histology or perform therapeutic

endoscopic interventions using VCE. In contrast, DBE provides higher-resolution imaging with improved visualization because of the capability to insufflate air, irrigate, and suction obscuring mucus/material and the ability to perform a focused examination of any abnormality visualized. This technique also allows clinicians to obtain tissue samples, making treatment of the entire SB possible in a clinical setting.[11–13]

It has also a high diagnostic yield for occult gastrointestinal bleeding (OGIB), when the SB is suggested to be the source of bleeding by VCE or DBE.[14] However, only a few descriptions of the endoscopic findings or specific bleeding sources discovered in the SBs of patients with PH are available.[6,15] None of these studies has utilized DBE to assess the incidence and characteristics of the SB abnormalities seen in patients with PH. We sought to use DBE to define the endoscopic findings present in the SB of patients with PH and to determine if these findings are associated with specific clinical characteristics. We also evaluated the availability of DBE for endoscopic therapy and the associated complications.

Patients and methods

Patients

This study was a nonrandomized, retrospective analysis of patients with PH caused by cirrhosis or extrahepatic portal vein obstruction (EHO) who were examined by DBE at Miyazaki Medical Center Hospital between September 2004 and March 2007. We confirmed the presence of liver cirrhosis by compatible physical examination, laboratory findings, histology, or radiographic features. EHO was diagnosed in patients with PH who had normal liver function tests, no clinical signs of cirrhosis, and compatible radiographic findings. PH was diagnosed by endoscopic or radiographic evidence of esophageal, gastric, or intraabdominal varices with or without splenomegaly. The severity of cirrhosis was graded using the Child-Pugh classification.

A total of 24 procedures in 15 consecutive patients with PH (12 men, 3 women; mean age, 65.8 ± 8.7 years; age range, 48–75 years) were performed. Oral, anal, and combined approaches were performed in 2, 8, and 5 patients, respectively. One patient required 5 procedures; the anal approach had to be repeated in 1 patient. We compared these results to those for 90 DBE procedures in 49 control patients (39 men and 10 women; mean age, 48.8 ± 21.1 years; age range, 16–85 years). In 49 control patients, 14 patients underwent DBE for OGIB, 10 for abdominal pain, 8 for ileus, 7 for inflammatory bowel disease, 3 for diarrhea, 2 for suspicion of tumor, 2 for fever of unknown etiology, 2 for inability to perform an endoscopic retrograde cholangiopancreatography because of previously manipulated intestines, and 1 for suspicion of infection. Patients who did not have chronic liver disease or PH who were treated at our hospital served as controls. Oral, anal, and combined approaches were performed for 7, 22, and 20 of the control patients, respectively, which includes several who were subjected to repeated procedures. Written informed consent for examination by DBE was obtained from all patients.

Methods of double balloon endoscopy

The double balloon endoscopic system (Fujinon EN-450T5/W; Fujinon, Saitama, Japan) utilizes a video endoscope with a working length of 200 cm and a flexible single-use overtube with a length of 145 cm (including the balloon). The double balloon technique has been described previously.[10] During withdrawal, administration of hyoscine butylbromide or glucagon reduces peristalsis in the SB, optimizing visualization. Sodium picosulfate is given 1 day before examination; no other specific preparation is required for an oral approach. For retrograde enteroscopy from an anal approach, bowel cleansing was performed as for colonoscopy. Therapeutic procedures were performed through a working channel. Argon plasma beam-directed coagulation (APC; 1.2 l/min/max, 35 W; ERBE 300 series, Tubigen, Germany) was used in the subset of cases in which bleeding sources were identified.

Classification of endoscopic abnormalities in the small bowel in patients with portal hypertension

The data collected for each patient included age, gender, etiology of cirrhosis, Child-Pugh class, and gastrointestinal tract abnormalities identified by upper and lower endoscopy. We evaluated each patient for any evidence of varices in the esophagus, stomach, colon, or anorectum and for changes indicative of PHG or portal hypertensive colopathy (PHC). PHG was diagnosed following recognition of elementary lesions, such as a mosaic-like pattern, red-point lesions, cherry-red spots, or black-brown spots.[7] The colonic abnormalities seen endoscopically in PHC are similar to those seen in PHG, including diffuse hyperemia and edema resembling chronic colitis, angiodysplasia-like lesions, patchy hyperemic lesions, a severe colitis-like appearance, and spontaneous bleeding from the mucosa.[7,8] The abnormal endoscopic findings seen by DBE in patients with PH, which were definitive for PHE, were divided into two categories: villous abnormalities and vascular lesions. Villous abnormalities included edema, atrophy, and reddening

of villi. Angiodysplasia-like lesions, dilated/proliferated vessels, and varices comprised the vascular lesions. A finding of each of these lesions was scored as a point, to provide a final score with a maximum of six points. The angiodysplasia-like lesions were subclassified as red spots, vascular spiders, and lymphoid follicles with dilated vessels. Dilated/proliferated vessels were further subclassified into tree-like dilated vessels and coil-like fine vessels.

Diagnosis for source of occult gastrointestinal bleeding

Patients with positive fecal occult blood and/or iron deficiency anemia with negative upper endoscopy and colonoscopy were defined as having OGIB.[16] Before DBE, all patients with OGIB were evaluated within 1 month by upper endoscopy and colonoscopy. For patients with OGIB, endoscopic findings by DBE were classified as positive (diagnostic), suspicious, or negative (failed).[17] Findings were classified as positive if the observed findings could explain the signs/symptoms of the patient. These findings typically helped to determine further management or were confirmed by other modalities. Findings were considered suspicious if an observed finding failed to explain completely the signs/symptoms of the patient, necessitating further investigation to evaluate its clinical relevance. When no abnormality could be detected despite clinical indication of an existing lesion, findings were considered to be negative.

Clinical characteristics and endoscopic abnormalities that we defined as portal hypertensive enteropathy

We compared the clinical characteristics and prevalence of PHE-defining endoscopic abnormalities between patients with PH and those without chronic liver disease (control patients). We also calculated the number of abnormal findings in 13 patients with liver cirrhosis. We compared patients with four or more findings of PHE to those with fewer than four findings to determine if this calculated score correlated with the severity of liver disease, the presence of esophagogastric varices (EGV), PHG, PHC, or other clinical characteristics.

Statistical analysis

All statistical analyses were performed using Statview J-4.5 software (Abacus Concepts, Berkeley, CA, USA) or SPSS (Chicago, IL, USA). Data are shown as the means (± SD). Comparisons were performed using the Mann–Whitney U test, Fisher's exact test, or the χ^2 test, as appropriate. Differences were considered statistically significant when the P value was less than 0.05.

Results

Prevalence and endoscopic findings of portal hypertensive enteropathy

The characteristics of 15 patients with PH and 49 control patients evaluated by DBE are detailed in Table 1. The average age of patients and the frequency of OGIB as an indication for DBE in patients with PH were higher than those for control patients. Several laboratory values, including platelet counts, serum albumin, and bilirubin, were also significantly different between the two groups. In contrast, the levels of serum alanine transferase (ALT) did not differ between the two groups.

Fourteen of the 15 patients exhibited villous abnormalities, including edema (Fig. 1A), atrophy (Fig. 1B), or reddening (Fig. 1C) of villi. All 15 patients with PH displayed vascular lesions, including angiodysplasia-like abnormalities [Fig. 2A-(1), -(2), or -(3)], dilated/proliferating vessels [Fig. 2B-(1) or -(2)], or varices (Fig. 2C). Thus, although endoscopic abnormalities were observed in the SB of all patients with PH, there were no villous abnormalities or vascular lesions in control patients.

The association between portal hypertensive enteropathy-defining abnormal findings and clinical characteristics

The etiology of the PH was liver cirrhosis in 13 patients and EHO without cirrhosis in 2 patients (see Table 1). By DBE, 14 of the 15 patients with PH exhibited villous abnormalities, while vascular lesions were observed in all (Table 2). We sought to evaluate the correlation between these endoscopic abnormalities, which we considered to be associated with PH, and clinical parameters in the 13 patients with PH caused by cirrhosis. We compared patients with four or more positive findings of PHE to those with fewer than four positive findings to determine if PHE was associated with liver disease severity or with specific endoscopic findings of the upper or lower gastrointestinal tract (Table 3). PHE was unrelated to patient age, the presence of PHG or PHC, or severity of EGV. In addition, PHE did not correlate with any laboratory findings. The frequency of ascites in patients with high PHE scores, however, was significantly higher than that seen in those with low scores ($P = 0.02$).

Diagnostic findings in small bowel by double balloon endoscopy

We assessed the number of PHE-determining findings, diagnostic rates of small intestinal bleeding, and complications of DBE (Table 4). The frequency of

Table 1. Demographic, clinical, and endoscopic parameters of patients

Parameter	Patients with portal hypertension	Control patients	*P* value*
Patients (procedures)	15 (24)	49 (90)	–
Age (mean ± SD; years)	65.8 ± 8.7	48.8 ± 21.1	<0.01
Sex (male/female)	12/3	39/10	>0.99
Indications for double balloon endoscopy			
OGIB/ileus/other	13/1/1	14/8/27	<0.001
Etiology of portal hypertension			
Cirrhosis	13	0	–
Etiology (HBV/HCV/alcohol/unknown)	1/5/4/3	—	–
Child-Pugh class (A/B/C)	1/12/0	—	–
Extrahepatic portal vein obstruction	2	0	–
Presence of esophagogastric varices	9	0	–
Presence of portal hypertensive gastropathy	10	0	–
Presence of portal hypertensive colopathy	9	0	–
Presence of anorectal varices	8	0	–
Ascites	5	0	–
Platelet ($\times 10^4$/mm^3)	12.7 ± 11.7	24.8 ± 8.9	<0.001
Serum albumin (g/dl)	3.0 ± 0.6	3.9 ± 0.6	<0.001
Total bilirubin (mg/dl)	0.9 ± 0.4	0.6 ± 0.4	<0.01
ALT (IU/l)	28.3 ± 18.9	28.8 ± 22.1	0.91

OGIB, obscure gastrointestinal bleeding
* Comparisons were performed with the Mann–Whitney *U* test, Fisher's exact test, or the χ^2 test, as appropriate

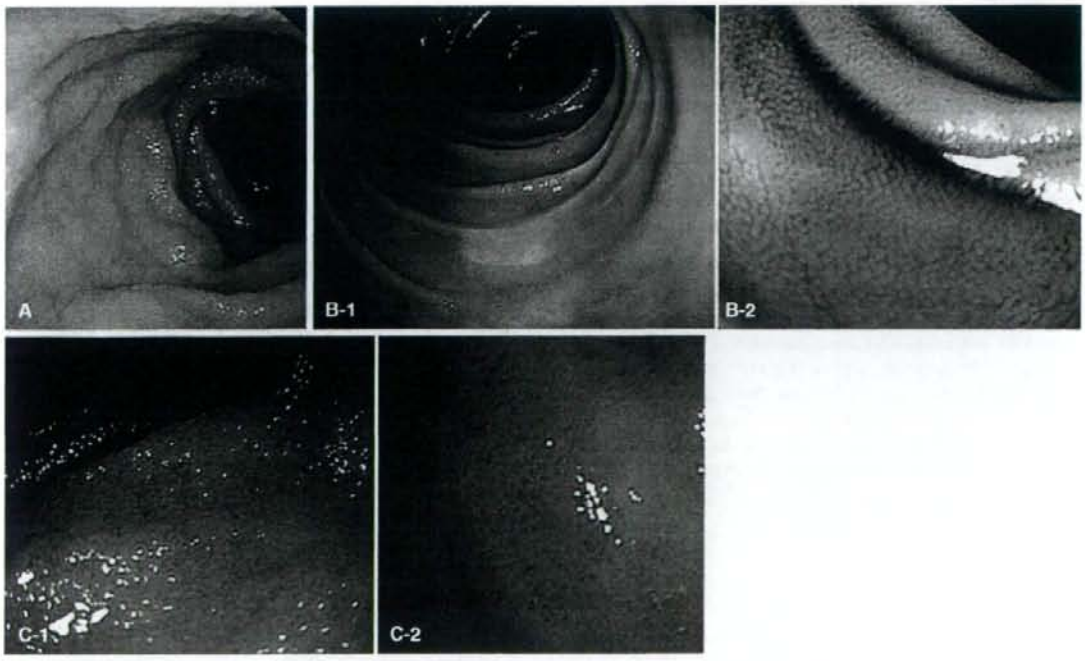

Fig. 1. Three different types of villous abnormalities were seen in the small bowel of patients with portal hypertension: edema of villi (**A**); atrophy of villi (**B-1**, **B-2**); reddening of villi (**C-1**, **C-2**)

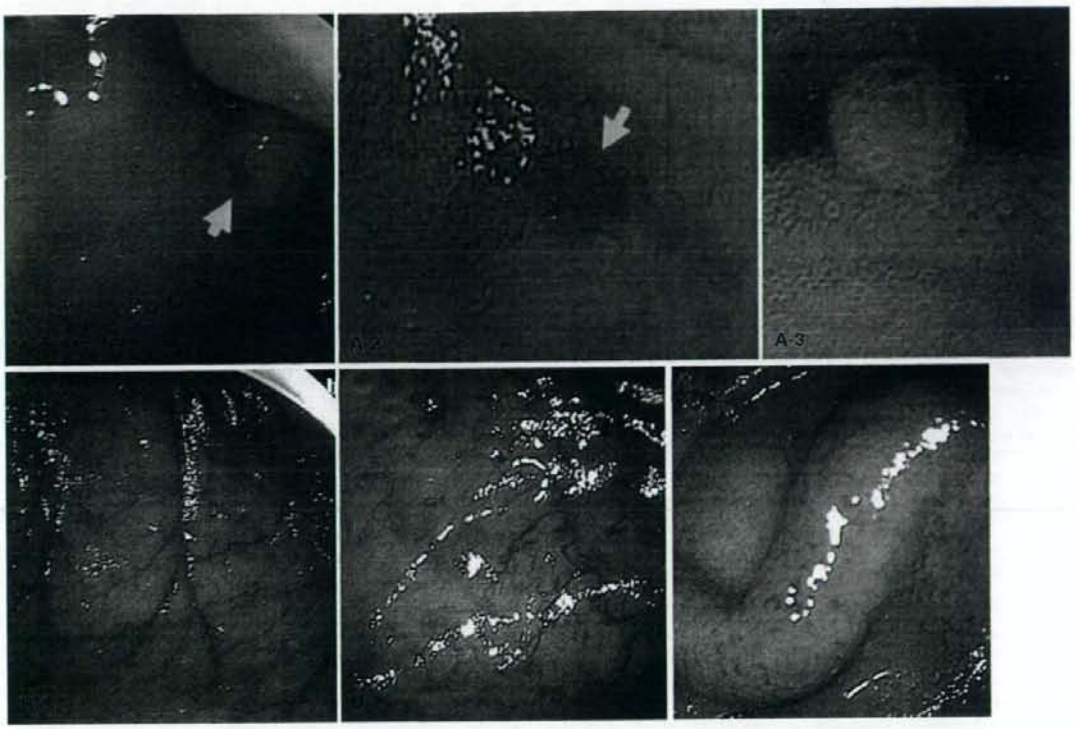

Fig. 2. Three different types of vascular lesions, including angiodysplasia-like lesions (**A**), dilated/proliferated vessels (**B**), and varices (**C**), were seen in the small bowel of patients with portal hypertension. **A-1**, red spots (*arrow*); **A-2**, vascular spiders (*arrow*); **A-3**, lymphoid follicles with dilated vessels; **B-1**, tree-like dilated vessels; **B-2**, coil-like fine vessels; **C**, varices

Table 2. Classification and frequency of the endoscopic findings of portal hypertensive enteropathy

Endoscopic findings	$n = 15$ (%)
1. Villous abnormalities	14 (93%)
A. Edema of villi	11 (73%)
B. Atrophy of villi	6 (40%)
C. Reddening of villi	7 (47%)
2. Vascular lesions	15 (100%)
A. Angiodysplasia-like lesions	10 (67%)
(1) Red spots	9 (60%)
(2) Vascular spiders	2 (13%)
(3) Lymphoid follicles with dilated vessels	2 (13%)
B. Dilated/proliferated vessels	14 (93%)
(1) Tree-like dilated vessels	12 (80%)
(2) Coil-like fine vessels	2 (13%)
C. Varices	1 (7%)

endoscopic abnormalities in the SB, which were diagnostic of PHE, was significantly higher in patients with PH than that seen in control patients. Definitive or suspicious bleeding sources, however, were observed in 69% (9/13) of patients with PH and 50% (7/14) of control patients; this diagnostic rate was not significantly different between the two groups of patients with OGIB. Bleeding sources identified included angiodysplasia-like lesions in the SB in 5 patients with PH, in whom 3 were definitive and 2 were suspicious. We identified

Table 3. The association of the number of positive portal hypertensive enteropathy-associated findings in patients with cirrhosis and other clinical features

	Number of positive findings of portal hypertensive enteropathy		
	4–6	0–3	*P* value*
Patients	6	7	
Age (mean ± SD; years)	71.0 ± 3.8	66.3 ± 7.1	0.28
Sex (male/female)	5/1	6/1	>0.99
Etiology (HBV/HCV/alcohol/uknown)	0/2/2/2	1/3/2/1	0.69
Child-Pugh class (A/B/C)	1/5/0	0/7/0	0.46
Presence of esophagogastric varices	2 (33%)	5 (71%)	0.29
Presence of portal hypertensive gastropathy	5 (83%)	5 (71%)	>0.99
Presence of portal hypertensive colopathy	2 (33%)	6 (86%)	0.10
Presence of anorectal varices	2 (33%)	4 (57%)	0.59
Presence of ascites	4 (67%)	0 (0%)	0.02
Prothrombin time (%)	72.7 ± 17.0	65.3 ± 15.3	0.32
Platelet ($\times 10^4/mm^3$)	11.1 ± 8.5	7.0 ± 2.7	0.32
Serum albumin (g/dl)	2.8 ± 0.5	2.8 ± 0.3	0.67
Total bilirubin (mg/dl)	0.9 ± 0.5	0.8 ± 0.4	>0.99
Alanine aminotransferase (IU/l)	34.3 ± 23.4	26.4 ± 17.2	0.62
Complication associated with double balloon endoscopy	3 (50%)	3 (43%)	>0.99

*Comparisons were performed with the Mann–Whitney *U* test, Fisher's exact test, or the χ^2 test, as appropriate

Table 4. Comparison of patients with and without portal hypertension

	Patients with portal hypertension	Control patients	*P* value*
Patients (procedures)	15 (24)	49 (90)	
Presence of portal hypertensive enteropathy	15 (100%)	0 (0%)	<0.001
Diagnostic rates of small intestinal bleeding (positive/suspicious/negative)[a]	7/2/4	5/2/7	0.57
Complications	7/24 (29%)	2/90 (2%)	<0.001

[a] In patients with obscure gastrointestinal bleeding
*Comparisons were performed with the Mann–Whitney *U* test, Fisher's exact test, or the χ^2 test, as appropriate

jejunal varices in 1 patient, a SB ulcer in 1, a SB diverticulum in 1, and duodenal varices in 1. Of these abnormalities, the varices are likely associated with PH, whereas the SB ulcer and diverticulum may not be associated. The duodenal varices were excluded from the findings of PHE in this study (see Table 2). The bleeding sources in control patients included a duodenal ulcer in 1 patient, SB ulcers in 5 patients, and SB angiodysplasia in 1 patient.

Treatment in small bowel by double balloon endoscopy or complications associated with its use

Endoscopic treatments using DBE were performed in three patients with endoscopic abnormalities in the SB. One patient received APC treatment for angiodysplasia-like lesions, one patient was treated with clipping and APC for angiodysplasia-like lesions, and a third was treated with clipping of lymphoid follicles with dilated vessels. Seven of 24 or 2 of 90 procedures in patients with or without PH, respectively, developed fevers (temperatures higher than 37.5°C) in the first 24 h after procedure (Table 4). The difference in frequency was statistically significant between the two groups ($P < 0.001$). Although aspiration pneumonia was suspected to occur in one of the patients with PH, the causes of fever in the other patients were not clear. Antibiotic therapy, however, was not necessary except for the one patient with pneumonia. There were no severe complications, excluding pneumonia, in either group with or without endoscopic treatment.

Discussion

Currently, there is no classification system with which to grade the severity of endoscopic abnormalities in cirrhotic patients with PHE. De Palma et al. proposed that PHE lesions be classified into two categories, mucosal inflammatory-like abnormalities (edema, ery-

thema, granularity, and friability) and vascular lesions (cherry-red spots, telangiectasias, angiodysplasia-like lesions, and varices).[15] Rana et al. defined the diagnosis of ileopathy as the presence of lesions similar in appearance to spider angioma, diffuse or patchy regions of hyperemia, cherry-red spots, and prominent veins.[8] Although we did not investigate the histology of mucosal lesions in this study, we classified the endoscopic findings in the SB of patients with PH into two categories, villous abnormalities and vascular lesions. We also subclassified the findings in these two categories and calculated the total number of positive findings in these six subcategories (see Table 2). Although it is unclear if these findings were specific for PHE, our observations indicated their prominence in patients with PH. Further studies are required to improve the classification and scoring system proposed in this report.

De Palma et al. reported that 68% of cirrhotic patients with PH were found to have PHE evaluated by VCE.[15] Endoscopic abnormalities in the ileum were noted in 13 of 38 patients examined (34%).[8] In contrast, we report that all patients with PH were observed to have at least one abnormal finding in the SB considered to be associated with PH. The high percentage likely correlates with the finding that 13 of the 15 patients with PH had evidence of OGIB with negative findings on upper and lower endoscopies. Previously reported prevalences of PHC vary from 37% to 70%, likely because of the heterogeneity of patients.[18-20] The limitations of studies, including our report, examining patients with PHE are the small number of patients with PH. In addition, although it would be better to compare the results of VCE and DBE in this study, we unfortunately did not have data for VCE. Further studies with larger numbers of patients will be needed to determine accurately the frequency of PHE as assessed by DBE and VCE.

One of the main causes of death for patients with PH is gastrointestinal bleeding. Portal hypertensive gastrointestinal vasculopathy, which can occur throughout the esophagus, stomach, and colon, is typically the origin of bleeding in patients with PH. PHE secondary to PH, especially the presence of varices in the SB, may also be a common source of bleeding.[15,21,22] There are no data, however, detailing that abnormal findings in the SB has any impact on the clinical treatment of PH, with the exception of cases with OGIB. Prospective observation should reveal the impact of PHE in cases without OGIB.

De Palma et al. initially demonstrated that 25 of 37 (68%) patients with cirrhosis and PH also had PHE and that the prevalence of PHE increased with worsening Child-Pugh class; 32% of patients with PHE were Child-Pugh class C, while only 9% of those without PHE were Child-Pugh class C.[15] PHE was also significantly associated with 2+ or larger esophageal varices, PHG, and PHC. Repici et al., however, found no correlation between the presence of PHE and Child-Pugh score, the size of varices, or the presence of PHG or PHC.[23] In this study, all patients with PH had evidence of PHE. We attempted to correlate the number of positive PHE-associated findings with laboratory findings. Our comparison of cirrhosis patients with at least four positive findings of PHE with those exhibiting fewer than four such findings demonstrated that laboratory findings, such as serum albumin, were not significantly different between the two groups. In addition, neither esophagogastric varices, PHG, PHC, nor anorectal varices correlated with PHE. The number of positive findings of PH, however, was associated with presence of ascites (see Table 3). The mechanism by which ascites develops in patients with cirrhosis is multifactorial, with the largest contribution from severe sinusoidal PH. Thus, the pathophysiology supports the association of PH with our PHE scoring system. Large prospective studies are required to evaluate the clinical significance of SB mucosal changes in patients with PH in the presence or absence of cirrhosis.

The complication rate of DBE is approximately 1%.[24,25] While perforation is a rare complication associated with DBE, no severe complications occurred in this study. Our study indicates, however, that postprocedure fever induced by DBE was more common in patients with PH than in those without PH. This complication may be associated with bacterial translocation, which typically occurs in patients with liver cirrhosis.[26,27] Comparison of cirrhotic patients with and without complications did not reveal any association of the incidence of complications with the severity of liver damage. In addition, the median time of the DBE procedure did not correlate with the incidence of complications (data not shown). In contrast, no complications were observed in the two EHO patients with PH. As the small number of EHO patients is insufficient to reveal any association, further examination will be required.

As DBE is contraindicated in patients with esophageal varices, because of an increased risk of rupture, VCE is the first diagnostic step for PHE in patients with PH. Performing DBE, however, is reasonable to examine the SB in patients with PH, as it provides a high diagnostic yield and the capability to perform therapeutic interventions. The small vascular lesions characteristic of PHE may only rarely be the sources of OGIB in patients with PH. After the bleeding has stopped, it is difficult to identify these sources of bleeding in patients with PHE as these vascular lesions are tiny. In cases in which bleeding is suspected in the SB, the diagnostic rate identifying the source of bleeding was higher in cases that underwent DBE within three days of the bleeding episode than in those who were evaluated after 1 to 2 weeks (unpublished data). Thus,

we propose that DBE should be used to examine the SB in OGIB patients with PH, especially within the first 3 days after bleeding.

Currently, there are no data evaluating the treatment of the SB using DBE in patients with PHE. The thin intestinal wall of the SB makes it difficult to perform sclerotherapy and ligation, the standard treatments for esophageal, gastric, and rectal varices. DBE, in contrast to VCE, does facilitate concurrent diagnosis and treatment. As clinical use of DBE for diagnosis and treatment of PHE is still new, future studies will be needed to define the role of DBE in this disease.

References

1. Groszmann RJ, Abraldes JG. Portal hypertension: from bedside to bench. J Clin Gastroenterol 2005;39(suppl 2):S125–30.
2. Gupta TK, Chen L, Groszmann RJ. Pathophysiology of portal hypertension. Clin Liver Dis 1997;1:1–12.
3. Lebrec D, Benhamou J-P. Ectopic varices in portal hypertension. Clin Gastroenterol 1985;14:105–21.
4. Salam AA, Goldman M, Smith D Jr, Hill HL. Gastric, intestinal, and gallbladder varices: hemodynamic and therapeutic considerations. South Med J 1979;72:402–8.
5. Gappell MS, Price JB. Characterization of the syndrome of small and large intestinal variceal bleeding. Dig Dis Sci 1987;32:422–7.
6. Jacob P, Favre O, Daudet J, Lapalus M, Soussan EB, Saurin J. Clinical impact of capsule endoscopy for unexplained bleeding in cirrhosis; results from 21 patients. Endoscopy 2005;37(suppl 1): A287.
7. Rondonotti E, Villa F, Signorelli C, Franchis RD. Portal hypertensive enteropathy. Ganstrointest Endoscopy Clin N Am 2006;16: 277–86.
8. Rana S, Bhasin DK, Jahagirdar S, Raja K, Nada R, Kochhar R, et al. Is there ileopathy in portal hypertension? J Gastroenterol Hepatol 2006;21:392–7.
9. Iddan G, Meron G, Glukhovsky A, Swain P. Wireless capsule endoscopy. Nature 2000;405:417.
10. Yamamoto H, Sekine Y, Sato Y, Higashizawa T, Miyata T, Iino S, et al. Total enteroscopy with a nonsurgical steerable double balloon method. Gastrointest Endosc 2001;53:216–20.
11. Di Caro S, May A, Heine DG, Heine DG, Fini L, Landi B, et al. The European experience with double balloon enteroscopy: indications, methodology, safety, and clinical impact. Gastrointest Endosc 2005;62:545–50.
12. Yamamoto H, Sugano K. A new method of enteroscopy: the double balloon method. Can J Gastroenterol 2003;17:273–4.
13. Sun B, Rajan E, Cheng S, Shen R, Zhang C, Zhang S, et al. Diagnostic yield and therapeutic impact of double balloon enteroscopy in a large cohort of patients with obscure gastrointestinal bleeding. Am J Gastroenterol 2006;101:2011–5.
14. Hadithi M, Heine GD, Jacobs MA, van Bodegraven AA, Mulder CJ. A prospective study comparing video capsule endoscopy with double balloon enteroscopy in patients with obscure gastrointestinal bleeding. Am J Gastroenterol 2006;101:52–7.
15. De Palma G, Rega M, Masone S, Persico F, Siciliano S, Patrone F, et al. Mucosal abnormalities of the small bowel in patients with cirrhosis and portal hypertension: a capsule endoscopy study. Gastrointest Endosc 2005;62:529–34.
16. Zuckerman GR, Prakash C, Askin MP, Lewis BS. AGA technical review on the evaluation and management of occult and obscure gastrointestinal bleeding. Gastroenterology 2000;118:201–21.
17. Costamagna G, Shah SK, Riccioni ME, Foschia F, Mutiqnani M, Perri V, et al. A prospective trial comparing small bowel radiographs and video capsule endoscopy for suspected small bowel disease. Gastroenterology 2002;123:999–1005.
18. Ghoshal UC, Biswas PK, Roy G, Pal BB, Dhar K, Banerjee PK. Colonic mucosal changes in portal hypertension. Trop Gastroenterol 2001;22:25–7.
19. Ito K, Shiraki K, Sakai T, Yoshimura H, Nakano T. Portal hypertensive colopathy in patients with liver cirrhosis. World J Gastroenterol 2005;11:3127–30.
20. Kozarek RA, Botoman VA, Bredfeldt JE, Roach JM, Patterson DJ, Ball TJ. Portal colopathy: prospective study in patients with portal hypertension. Gastroenterology 1991;101:1192–7.
21. Jimenez-Saenz M, Romero-Vazquez J, Caunedo-Alvarez A, Herrerias-Gutierrez JM. Capsule endoscopy: a useful tool in portal hypertensive enteropathy. Gastrointest Endosc 2006;64: 152.
22. Tang SJ, Zanati S, Dubcenco E, Cirocco M, Christodoulou D, Kandel G, et al. Diagnosis of small bowel varices by capsule endoscopy. Gastrointest Endosc 2004;60;129–35.
23. Repici A, Pennazio M, Ottobrelli A, Barbon V, De Angelis C, De Lio A, et al. Endoscopic capsule in cirrhotic patients with portal hypertension: spectrum and prevalence of small bowel lesions. Endoscopy 2005;37(suppl 1):A72.
24. Yamamoto H, Kita H, Sunada K, Hayashi Y, Sato H, Yano T, et al. Clinical outcomes of double balloon endoscopy for the diagnosis and treatment of small-intestinal diseases. Clin Gastroenterol Hepatol 2004;2:1010–6.
25. May A, Nachbar L, Ell C. Double balloon enteroscopy (push-and-pull enteroscopy) of the small bowel: feasibility and diagnostic and therapeutic yield in patients with suspected small bowel disease. Gastrointest Endosc 2005;62:62–70.
26. Cirera I, Bauer TM, Navasa M, Vila J, Grande L, Taura P, et al. Bacterial translocation of enteric organisms in patients with cirrhosis. J Hepatol 2001;34:32–7.
27. Francés R, Rodríguez E, Muñoz C, Zapater P, De la ML, Ndongo M, et al. Intracellular cytokine expression in peritoneal monocyte/macrophages obtained from patients with cirrhosis and presence of bacterial DNA. Eur J Gastroenterol Hepatol 2005;17:45–51.

Tumor cell apoptosis induces tumor-specific immunity in a CC chemokine receptor 1- and 5-dependent manner in mice

Noriho Iida,* Yasunari Nakamoto,* Tomohisa Baba,† Kaheita Kakinoki,* Ying-Yi Li,† Yu Wu,† Kouji Matsushima,‡ Shuichi Kaneko,* and Naofumi Mukaida†,1

*Disease Control and Homeostasis, Graduate School of Medical Science, and †Division of Molecular Bioregulation, Cancer Research Institute, Kanazawa University, Kanazawa, Japan; and ‡Department of Molecular Preventive Medicine, School of Medicine, University of Tokyo, Tokyo, Japan

Abstract: The first step in the generation of tumor immunity is the migration of dendritic cells (DCs) to the apoptotic tumor, which is presumed to be mediated by various chemokines. To clarify the roles of chemokines, we induced apoptosis using suicide gene therapy and investigated the immune responses following tumor apoptosis. We injected mice with a murine hepatoma cell line, BNL 1ME A.7R.1 (BNL), transfected with HSV-thymidine kinase (tk) gene and then treated the animals with ganciclovir (GCV). GCV treatment induced massive tumor cell apoptosis accompanied with intratumoral DC infiltration. Tumor-infiltrating DCs expressed chemokine receptors CCR1 and CCR5, and T cells and macrophages expressed CCL3, a ligand for CCR1 and CCR5. Moreover, tumor apoptosis increased the numbers of DCs migrating into the draining lymph nodes and eventually generated a specific cytotoxic cell population against BNL cells. Although GCV completely eradicated HSV-tk-transfected BNL cells in CCR1-, CCR5-, or CCL3-deficient mice, intratumoral and intranodal DC infiltration and the subsequent cytotoxicity generation were attenuated in these mice. When parental cells were injected again after complete eradication of primary tumors by GCV treatment, the wild-type mice completely rejected the rechallenged cells, but the deficient mice exhibited impairment in rejection. Thus, we provide definitive evidence indicating that CCR1 and CCR5 and their ligand CCL3 play a crucial role in the regulation of intratumoral DC accumulation and the subsequent establishment of tumor immunity following induction of tumor apoptosis by suicide genes. *J. Leukoc. Biol.* 84: 1001–1010; 2008.

Key Words: *dendritic cells · gene therapy*

INTRODUCTION

Hepatocellular carcinoma (HCC) occurs in individuals with chronic liver disease related to hepatitis B or C virus infections [1–3]. Even after the curative treatments for HCC, such as surgical resection and radiofrequency ablation, tumor recurrence often occurs because of the multicentric development of HCC in the cirrhotic liver [4]. Immune-based therapies, particularly those based on dendritic cells (DCs), may be theoretically effective in preventing the recurrence because of their potential capacity to search for and eradicate tumor cells irrespective of site [5]. However, DC-based therapy is still considered to be in its infancy, probably as a result of the lack of effective techniques for enhancing the immune response to human cancer cells including HCC, which are generally poor in immunogenicity.

Apoptotic tumor cells are generally less immunogenic than necrotic cells, but they can sometimes induce efficient antitumor immune responses depending on the type of apoptosis inducer. Indeed, some anticancer drugs can induce apoptosis of tumor cells and simultaneously enhance the immunogenicity of apoptotic cancer cells [6–8]. Ganciclovir (GCV) can activate the protease family of caspases and induce apoptosis selectively in the cells transfected with the HSV-thymidine kinase (tk) gene [9, 10]. Thus, when GCV is administered systemically to tumor-bearing individuals, it induces apoptosis of HSV-tk-transfected tumor cells but not normal cells. This treatment strategy, designated as suicide gene therapy, can induce immunogenic apoptosis of the tumor cells [11], as evidenced by a massive intratumoral infiltration of macrophages and T cells [12]. Moreover, the expression of various proinflammatory cytokines is augmented at the tumor sites following GCV treatment [12, 13]. Furthermore, to enhance the suicide gene therapy-induced immune responses, the simultaneous use of cytokines such as GM-CSF, IL-2, and MCP-1/CCL2 has been used with some success [14–16]. To design more effective methods of preventing tumor recurrences, it is necessary to fully understand the immune responses after tumor apoptosis induced by HSV-tk/GCV suicide gene therapy.

DCs are potent APC that play a crucial role in the establishment of adoptive immune response. Immature DCs capture and process antigens at the inflammatory sites and thereafter migrate to the draining lymph node, where they

[1] Correspondence: Division of Molecular Bioregulation, Cancer Research Institute, Kanazawa University, 13-1 Takara-machi, Kanazawa 920-0934, Japan. E-mail: naofumim@kenroku.kanazawa-u.ac.jp

Received November 26, 2007; revised June 12, 2008; accepted June 30, 2008.

doi: 10.1189/jlb.1107791

undergo phenotypical and functional maturation. At the draining lymph node, the mature DCs interact with naïve T cells and present the captured and processed antigen to T cells [17, 18].

Chemokines are presumed to play an essential role in the regulation of DC trafficking and DC–T cell interaction in general [19–22]. Circulating immature DCs express inflammatory chemokine receptors such as CCR1, CCR2, CCR5, and CCR6, and these DCs can reach the source of the inflammatory stimulus under the guidance of the ligand gradient for the expressed receptors such as CCL2, CCL3, CCL4, CCL5, CCL7, and CCL20. After capturing antigens, DCs undergo maturation, resulting in a decrease in inflammatory chemokine receptor expression and a reciprocal increase in CCR7 expression. Mature DCs expressing CCR7 migrate to T cell-rich areas of the draining lymph nodes, where the ligands for CCR7, CCL19, and/or CCL21 are expressed abundantly. However, it still remains elusive whether similar mechanisms operate in the DC migration process following massive tumor apoptosis induced by treatments such as gene therapy, chemotherapy, and radiation therapy.

Here, we demonstrate the induction of specific tumor immunity by tumor apoptosis after HSV-tk/GCV suicide gene therapy and essential roles of DCs in this process. Moreover, we provide definitive evidence to indicate that CCR1 and CCR5 and their ligand CCL3 play a key role in the regulation of intratumoral DC accumulation and the subsequent establishment of tumor immunity following induction of tumor apoptosis by HSV-tk/GCV suicide gene therapy. These observations might lay the foundation for devising novel measures to enhance antitumor immune responses to prevent tumor recurrence.

MATERIALS AND METHODS

Mice

Specific pathogen-free, 7- to 9-week-old male BALB/c mice were purchased from Charles River Japan (Yokohama, Japan) and were designated as wild-type (WT) mice. CCL3-deficient [CCL3 knockout (CCL3KO)] mice were obtained from Jackson Laboratories (Bar Harbor, ME, USA). CCR1KO mice were a gift from Dr. Philip M. Murphy [National Institute of Allergy and Infectious Diseases, National Institutes of Health (NIAID, NIH), Bethesda, MD, USA]. CCR5KO mice were generated as described previously [23]. All mice were backcrossed to BALB/c mice for eight to 10 generations. All animal experiments were performed under specific pathogen-free conditions in accordance with the Guideline for the Care and Use of Laboratory Animals of Kanazawa University (Japan).

Tumor cell lines

A murine HCC cell line, BNL 1ME A.7R.1 (BNL), was cultured in DMEM (Sigma Chemical Co., St. Louis, MO, USA) containing 10% FBS (Gibco, Long Island, NY, USA). BNL cells were infected with the retroviral vector pG1Sv.Na harboring HSV-tk cDNA. The infected BNL cells were cultured in 10% FBS-containing DMEM in the presence of 400 μg/ml G418 (Gibco). The surviving cells were tested for sensitivity to GCV in vitro as described previously [24]. GCV-sensitive cells were designated as BNL-tk and were used in the experiments.

Apoptosis detection assay

After culturing for 1 day with 5 μg/ml GCV, BNL-tk cells were harvested, and phosphatidyl serine levels were determined by staining the cells with propidium iodide (PI) and the Annexin V-FITC apoptosis detection kit (Calbiochem, Darmstadt, Germany) according to the manufacturer's instructions. At least 50,000 stained cells were analyzed on a FACSCalibur system (BD Biosciences, San Diego, CA, USA) for each determination.

Tumor injection

Seven- to 9-week old male WT, CCR1KO, CCR5KO, and CCL3KO mice were inoculated s.c. into the left flank with 2×10^5 BNL-tk cells on Day 0. From Days 14 to 18 (5 consecutive days), 75 mg/kg GCV (i.p.) was administered daily (see **Fig. 1C**). Tumors were removed at the indicated time intervals for immunohistochemical analysis and quantitative real-time RT-PCR. In another series of experiments, WT, CCR1KO, CCR5KO, or CCL3KO mice were inoculated with 1.5×10^5 BNL-tk on Day 0. The mice were i.p.-injected with 75 mg/kg GCV from Days 2 to 5. The animals were then rechallenged s.c. with 1.0×10^5 BNL in their right flank on Day 18, after confirming that the primary tumors were eradicated completely (see Fig. 5A). Tumor sizes were evaluated twice each week using calipers, and tumor volume was calculated by the following formula: Tumor volume (mm^3) = (the longest diameter) × (the shortest diameter)^2/2.

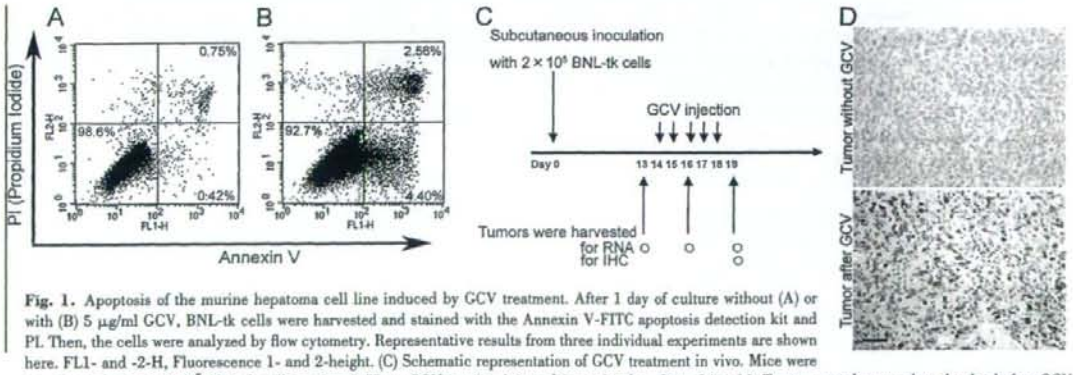

Fig. 1. Apoptosis of the murine hepatoma cell line induced by GCV treatment. After 1 day of culture without (A) or with (B) 5 μg/ml GCV, BNL-tk cells were harvested and stained with the Annexin V-FITC apoptosis detection kit and PI. Then, the cells were analyzed by flow cytometry. Representative results from three individual experiments are shown here. FL1- and -2-H, Fluorescence 1- and 2-height. (C) Schematic representation of GCV treatment in vivo. Mice were s.c.-injected with 2×10^5 BNL-tk cells on Day 0. Then, GCV was i.p.-injected into mice from Days 14 to 18. Tumors were harvested on the day before GCV injection (Day 13), on Day 3 or 6 after GCV injection (Day 16 or 19) for real-time RT-PCR analysis, and on Day 19 for immunohistochemistry (IHC). (D) Apoptotic cells detected in tumor tissues with or without GCV treatment using anti-ssDNA antibody. Original magnification, ×400. Original bar, 50 μm.

The draining lymph nodes (inguinal and axillary) were removed from the mice at the indicated time intervals for flow cytometric analysis and cytotoxicity assay.

Immunohistochemical analysis

Rabbit anti-mouse CCR5 polyclonal antibodies were prepared as described previously [25]. The removed tumor tissues were embedded in paraffin or the Sakura Tissue-Tek OCT compound (Sakura Finetek, Torrance, CA, USA) as frozen tissues. The paraffin-embedded sections were then stained with goat anti-mouse CCR1 (Santa Cruz Biotechnology, Santa Cruz, CA, USA), rabbit anti-CCR5, goat anti-mouse CCL3 (R&D Systems, Minneapolis, MN, USA), rat anti-mouse F4/80, anti-mouse CD3 (Serotec, Oxford, UK), rabbit anti-ssDNA, or rat anti-Ki67 (Dako Cytomation, Tokyo, Japan) overnight at 4°C. Cryostat sections of the frozen tissues were fixed with 4% paraformaldehyde (PFA) in PBS and stained with rat anti-mouse DEC205 (Serotec) or hamster anti-mouse CD11c (BD Biosciences) overnight at 4°C. The sections were then incubated for 1 h at room temperature with biotinylated rabbit anti-goat IgG, biotinylated swine anti-rabbit IgG, biotinylated rabbit anti-rat IgG (Dako Cytomation), or biotinylated mouse anti-hamster IgG (BD Biosciences). The immune complexes were visualized using a catalyzed signal amplification system (Dako Cytomation) or the ELITE avidin-biotin-peroxidase and diaminobenzidine substrate kits (Vector Laboratories, Burlingame, CA, USA), except for anti-ssDNA, where a novel HRP-labeled polymer (Envision$^+$, Dako Cytomation) was used, according to the manufacturer's instructions. As a negative control, goat IgG (R&D Systems), rabbit IgG (Dako Cytomation), rat IgG (Cosmo Bio, Tokyo, Japan), or hamster IgG (BD Biosciences) was used instead of specific primary antibodies. The numbers of positive cells were determined in each animal in 10 randomly chosen fields at 400-fold magnification by an examiner without any prior knowledge of the experimental procedures.

Double-color immunofluorescence analysis

Tumor tissues were embedded in paraffin or the OCT compound as frozen tissues. The paraffin-embedded sections were then stained with combinations of rat anti-mouse CD3 and goat anti-mouse CCL3 or anti-F4/80 and anti-CCL3 antibodies overnight at 4°C. After fixation with 4% PFA/PBS, cryostat sections were stained with the combinations rat anti-mouse CD4 (BD Biosciences) and anti-CCR1, rat anti-mouse CD8a (BD Biosciences) and anti-CCR1, anti-CD4 and anti-CCR5, anti-CD8a and anti-CCR5, rat anti-DEC205 and anti-CCR1, anti-DEC205 and anti-CCR5, PE-conjugated hamster anti-CD11c (BD Biosciences) and anti-CCR1, PE-conjugated anti-CD11c and anti-CCR5, PE-conjugated anti-CD11c and rat anti-CD11b (BD Biosciences), or PE-conjugated anti-CD11c and anti CD8a antibodies. After extensive washing, AF488 donkey anti-rat IgG (Invitrogen, Carlsbad, CA, USA) was applied as the secondary antibody to detect CD4-, CD8a-, CD3-, F4/80-, DEC205-, or CD11b-positive cells. Simultaneously, AF546 or AF488 donkey anti-goat IgG (Invitrogen) was used to detect CCR1- or CCL3-positive cells, and AF594 or AF488 donkey anti-rabbit IgG (Invitrogen) was used to detect CCR5-positive cells. The sections were observed using a confocal microscope (LSM 510 META, Zeiss, Thornwood, NY, USA). The percentage of double-positive cells was determined in each animal in five randomly chosen fields at 400-fold magnification by an examiner without any prior knowledge of the experimental procedures.

Flow cytometric analysis

Inguinal and axillary lymph nodes were removed and digested in a DNase I and collagenase solution (Sigma Chemical Co.). The resultant, single-cell preparations were stained with various combinations of FITC-labeled anti-CD4, FITC-labeled anti-CD86, PE-labeled anti-CD8, PE-labeled anti-CD11c, PE-labeled anti-CD44, and PE-labeled anti-CD62 ligand (CD62L) mAb (BD Biosciences). FITC-rat IgG, PE-hamster IgG, and PE-rat IgG were used as isotype controls (BD Biosciences). To prepare the tumor lysate, BNL or CT26 cells were suspended in PBS and subjected to four cycles of rapid freezing in liquid nitrogen and thawing at 55°C. The lysate was spun at 15,000 rpm to remove particulate cellular debris. To stain intracellular IFN-γ, the mononuclear cells harvested from the draining lymph nodes on Day 8 (see Fig. 5A) were incubated with the BNL or CT26 lysates at a tumor cell:mononuclear cell ratio of 1:1 in the presence of GolgiPlug (BD Biosciences). Six hours later, surface staining was performed with APC-conjugated CD8 antibodies. Intracellular IFN-γ was stained after fixation and permeabilization with BD Cytofix/Cytoperm buffer with PE-conjugated IFN-γ antibodies or isotype control using the Mouse Intracellular Cytokine Staining starter kit (BD Biosciences). At least 100,000 stained cells were analyzed on a FACSCalibur system for each determination. The data were expressed as a proportion of positive cells (compared with cells stained with an irrelevant control antibody), and the absolute positive cell numbers were calculated after determining the total cell numbers in the lymph nodes by the following formula: Absolute positive cell numbers = total cell number in the lymph nodes × percentage of positive cells × 1/100.

Quantitative real-time RT-PCR

Total RNA was extracted from the resected tumor and lymph nodes using RNA-Bee (Tel-Test, Friendswoods, TX, USA), according to the manufacturer's instructions. After the RNA preparations were further treated with RNase-free DNase I (Life Technologies, Gaithersburg, MD, USA) to remove residual DNA, cDNA was synthesized as described previously [26]. Quantitative real-time PCR was performed on an Applied Biosystems StepOne™ real-time PCR system (Applied Biosystems, Foster City, CA, USA) using the comparative threshold (C_T) quantification method. TaqMan® gene expression assays (Applied Biosystems) containing specific primers (Accession Numbers CCL3, Mm00441258_ml; CCL4, Mm00443111_m1; CCL5, Mm01302428_ml; CCR1, Mm00438260_s1; CCR5, Mm01216171_m1; GAPDH, Mm99999915_g1), TaqMan® minor groove binder probe (FAM™ dye-labeled), and TaqMan® fast universal PCR master mix were used with 10 ng cDNA to detect and quantify the expression levels of CCL3, CCL4, CCL5, CCR1, and CCR5. Reactions were performed for 20 s at 95°C and then for 40 cycles of 1 s at 95°C and 20 s at 60°C. GAPDH was amplified as an internal control. C_T values of GAPDH were subtracted from C_T values of the target genes (ΔC_T). ΔC_T values of tumors after GCV injection were compared with ΔC_T values of tumors before GCV injection.

Cytotoxicity assay

Mononuclear cells were isolated from the draining lymph nodes at the indicated time intervals and were incubated at a cell density of 2×10^6 cells/ml in the presence of 0.6×10^6 cells/ml BNL cells, which were irradiated at 50 Gy beforehand. After 5 days of culture, the cells were tested for cytotoxicity in a lactate dehydrogenase assay using the CytoTox 96 nonradioactive cytotoxicity assay kit (Promega, Madison, WI, USA), according to the manufacturer's instructions. Effector cells were added to target cells in triplicate at different E:T ratios. Percentage of specific lysis was calculated using the following formula: [(experimental−effector spontaneous−target spontaneous)/(target maximum−target spontaneous)] × 100%.

Adoptive transfer of DC

Draining lymph nodes were harvested on Day 8 (see Fig. 5A) and were digested with DNase I and collagenase solution. Mononuclear cells were obtained by centrifugation over a Histopaque-1077 density gradient (Sigma Chemical Co.), and DCs were isolated by CD11c-conjugated magnetic microbeads (Miltenyi Biotec, Auburn, CA, USA). CD11c-positive DCs (2.5×10^5/mouse) were injected into the left flank of GCV-treated KO mice on Day 8 (see Fig. 5A). On Day 18, DC-transferred mice were rechallenged with 1×10^5 BNL cells in their right flank, and tumor sizes were measured.

Statistical analysis

Data were analyzed statistically using one-way ANOVA followed by the Tukey-Kramer test, except for tumor progression data, which were analyzed using two-way ANOVA. Data of tumor sizes after adoptive transfer of the DC experiment were analyzed using the Mann-Whitney U test. $P < 0.05$ was considered statistically significant.

RESULTS

GCV treatment induces tumor cell apoptosis with intratumoral CCR1-, CCR5-, and CCL3-positive cell accumulation in WT mice

We investigated whether HSV-tk-GCV treatment can induce apoptosis in vitro in the tk-transfected murine hepatoma cell line BNL-tk. GCV treatment significantly increased the proportions of early (annexin-positive but PI-negative) and late (annexin-positive and PI-positive) apoptotic cells (Fig. 1, A and B). We injected GCV into WT mice i.p. after the s.c. BNL-tk tumor was formed macroscopically, according to the schedule, as shown in Figure 1C. Microscopic analysis revealed that more than half of the tumor cells were apoptotic and that a large number of mononuclear cells had accumulated in the tumor sites on Day 19 immediately following the completion of treatment (Fig. 1D and Supplemental Fig. 1). Thereafter, the tumor regressed macroscopically. We next investigated the chemokine receptor expression by tumor-infiltrating cells after the induction of in vivo tumor apoptosis by suicide gene therapy. Immunohistochemical analysis revealed the presence of few CCR1-, CCR5-, or CCL3-positive cells in tumors without GCV treatment (**Fig. 2A**). In contrast, GCV treatment caused intratumoral infiltration of a large number of CCR1-, CCR5-, and CCL3-positive cells in WT mice, along with massive apoptosis of tumor cells (Fig. 2A and Supplemental Fig. 2). The intratumoral mRNA expression of CCL3, CCL4, and CCL5 was markedly increased 3 days after GCV treatment, whereas that of their receptors CCR1 and CCR5 was augmented later than 3 days after GCV injection (Fig. 2B).

Tumor-infiltrating DCs express CCR1 and CCR5

To determine the type of tumor-infiltrating cells expressing CCR1, CCR5, or CCL3, we performed a double-color immunofluorescence analysis. CD4- and CD8-positive T cells expressed CCR5 but not CCR1 (**Fig. 3A** and Supplemental Fig. 3A; 78.2±8.9% of CD4-positive T cells and 92.6±8.2% of CD8-positive T cells expressed CCR5, and CCR1 was not detected in CD4- or CD8-positive T cells). In contrast, CD11c- and DEC205-positive cells, which infiltrated to tumor sites of WT mice after GCV treatment, expressed CCR1 and CCR5 (Fig. 3B and Supplemental Fig. 3B; 100% of CD11c-positive DCs expressed CCR1 and CCR5, 97.5±5.6% DEC205-positive cells expressed CCR1, and 100% DEC-positive cells expressed CCR5). Moreover, tumor-infiltrating, CD11c-positive DCs exhibited a "myeloid" phenotype, as 87.8 ± 14.8% of CD11c-positive cells expressed CD11b, and none of them expressed CD8a (Supplemental Fig. 3C). Furthermore, CCL3 proteins were detected in CD3-positive T cells, F4/80-positive macrophages (Fig. 3C; 72.0±9.1% of CD3-positive T cells and 87.0±12.0% of F4/80-positive macrophages expressed CCL3). These observations suggest that apoptosis induced by GCV treatment enhanced the expression of CCL3, CCL4, and CCL5 and then produced chemokines attracted to CD11c-positive DCs as well as CD3-positive T cells. To address this possibility, we investigated intratumoral infiltration of CD11c-positive DCs and CD3-positive T cells in CCR1KO, CCR5KO, or CCL3KO mice, which were s.c.-inoculated with 2×10^5 BNL-tk cells into WT and KO mice. The lack of CCR1, CCR5, or CCL3 had no discernible effects on the growth of primary tumors (**Fig. 4A**). Then, we injected GCV i.p. into the mice as shown in Figure 1C. Immunohistochemical analysis revealed

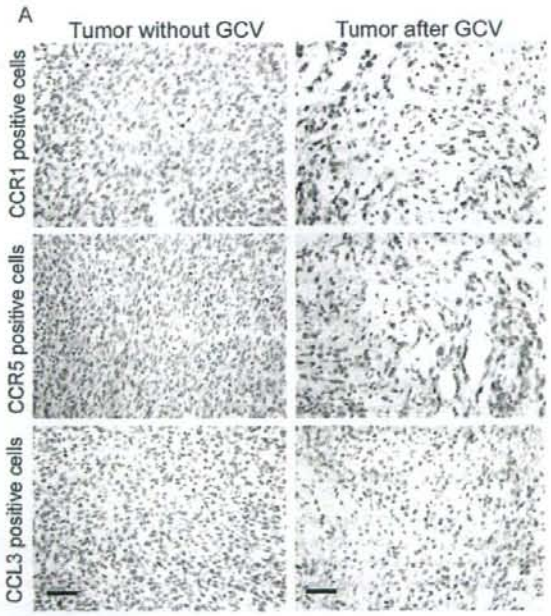

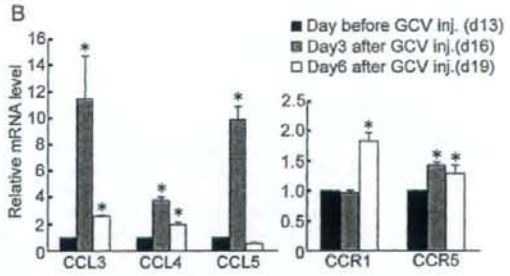

Fig. 2. Accumulation of tumor-infiltrating CCR1-, CCR5-, or CCL3-positive cells after tumor apoptosis induced by GCV treatment. Mice were inoculated with BNL-tk cells according to the schedule shown in Figure 1C. (A) Tumors were removed from WT mice on Day 19, and immunohistochemical analysis was performed using anti-CCR1, -CCR5, or -CCL3 antibody on tumors with or without GCV treatment. Representative results from three individual animals in each group are shown here. Original magnification, ×400. Original bars, 50 μm. (B) Real-time RT-PCR was performed on total RNA extracted from the tumor of WT mice harvested on Days 13, 16, or 19. The level of chemokine mRNA was normalized to GAPDH mRNA levels. Bars, ±1 SD ($n=3$); *, $P < 0.05$, compared with the day before GCV injection.

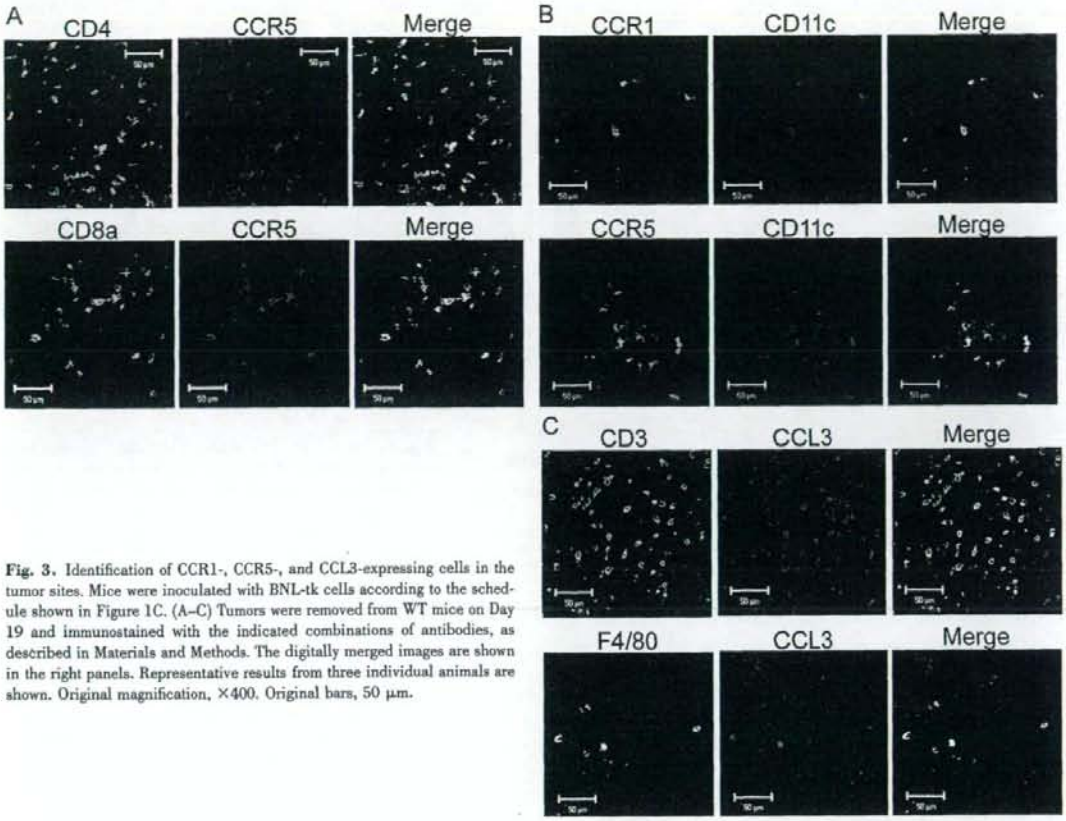

Fig. 3. Identification of CCR1-, CCR5-, and CCL3-expressing cells in the tumor sites. Mice were inoculated with BNL-tk cells according to the schedule shown in Figure 1C. (A–C) Tumors were removed from WT mice on Day 19 and immunostained with the indicated combinations of antibodies, as described in Materials and Methods. The digitally merged images are shown in the right panels. Representative results from three individual animals are shown. Original magnification, ×400. Original bars, 50 μm.

the presence of few CD3-, F4/80-, or DEC205-positive cells in tumors without GCV treatment (Fig. 4B). GCV treatment induced tumor cell apoptosis in CCL3KO, CCR1KO, and CCR5KO mice to a similar extent as that in WT mice (data not shown). Moreover, GCV treatment caused intratumoral accumulation of a large number of CD3-, CD4-, and CD8-positive T cells and DEC205- and CD11c-positive DCs in WT mice (Fig. 4, B and C). By contrast, the increases in intratumorally accumulating DEC205- and CD11c-positive cells and to a lesser extent, CD3-, CD4-, and CD8-positive cells were attenuated in CCR1KO, CCR5KO, and CCL3KO mice (Fig. 4, B and C). In contrast, GCV treatment induced intratumoral infiltration of F4/80-positive macrophages (Fig. 4B) and CD49b/DX5-positive NK cells (data not shown) in WT and KO mice to a similar extent.

Partial failure of CCR1KO, CCR5KO, and CCL3KO mice in rejecting the rechallenged tumor

Apoptosis induced by GCV treatment caused intratumoral infiltration of DCs and T cells in a CCR1- and/or CCR5-dependent manner. As intratumoral infiltration of DCs and T cells is a prerequisite for the establishment of specific tumor immunity, we examined the immune status of GCV-treated mice by rechallenging the parental BNL cell line. To completely eradicate the primary BNL-tk tumor, GCV was administered between 2 and 5 days after the tumor injection (**Fig. 5A**). Primary BNL-tk tumors were eradicated completely in WT, CCR1KO, CCR5KO, and CCL3KO mice at similar rates (data not shown). When these mice were injected again with parental BNL cells, WT mice rejected them completely. In contrast, CCR1KO, CCR5KO, and CCL3KO mice failed to completely eliminate the rechallenged tumor cells, although the growth rates were retarded in these mice compared with naïve WT mice (Fig. 5B). A marked cytotoxicity against BNL but not in CT26 cells was observed when draining lymph node-derived mononuclear cells of GCV-treated WT mice were used as effector cells. Only a modest amount of cytotoxicity was detected when mononuclear cells in the draining lymph nodes of GCV-treated CCR1KO, CCR5KO, or CCL3KO mice were used as effector cells (Fig. 5C). Further, GCV-induced tumor apoptosis enhanced the mRNA expression of Th1 cytokines such as IFN-γ, IL-12p40, and IL-18 in the draining lymph nodes of WT mice but not of CCR1KO, CCR5KO, and CCL3KO mice (Supplemental Fig. 4). Likewise, $CD8^+IFN\text{-}\gamma^+$ cells were increased markedly in GCV-treated WT mice when lymph node-derived mononuclear cells were cocultured with BNL cell lysates, compared with tumor-bearing or tumor-free

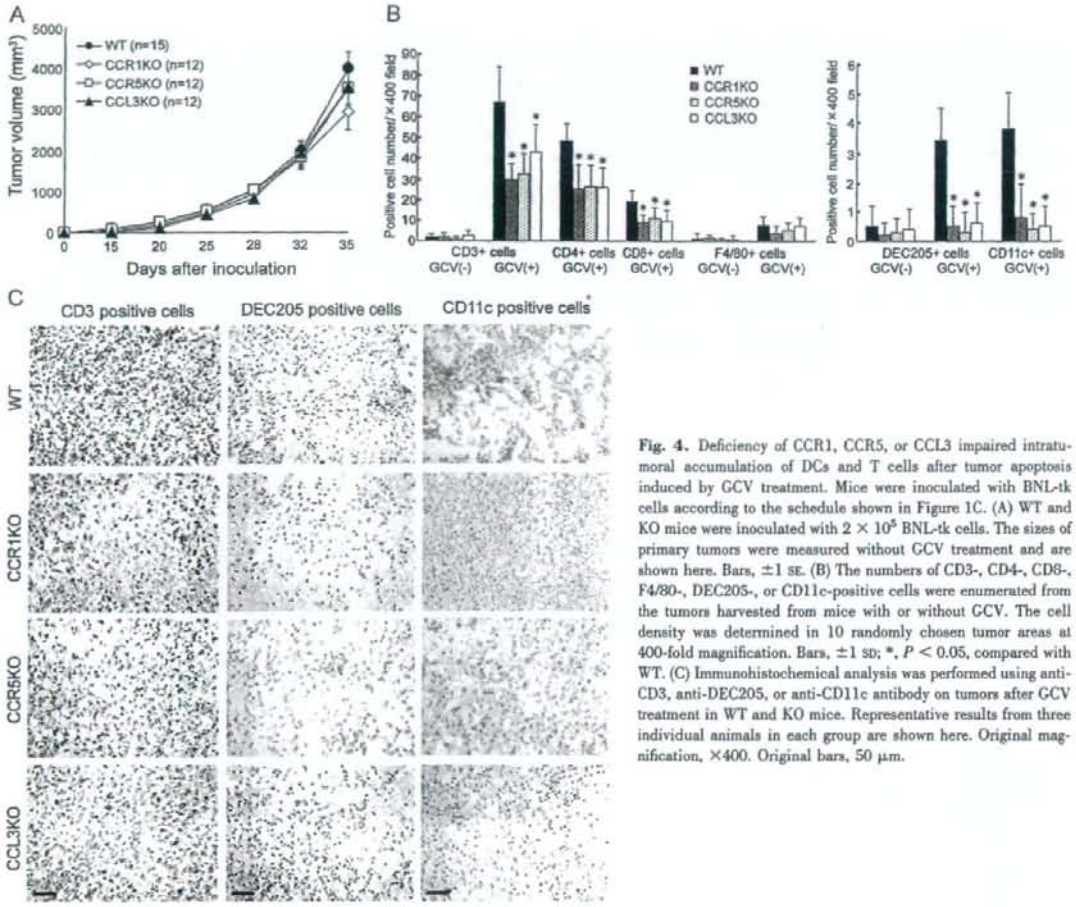

Fig. 4. Deficiency of CCR1, CCR5, or CCL3 impaired intratumoral accumulation of DCs and T cells after tumor apoptosis induced by GCV treatment. Mice were inoculated with BNL-tk cells according to the schedule shown in Figure 1C. (A) WT and KO mice were inoculated with 2×10^5 BNL-tk cells. The sizes of primary tumors were measured without GCV treatment and are shown here. Bars, ±1 SE. (B) The numbers of CD3-, CD4-, CD8-, F4/80-, DEC205-, or CD11c-positive cells were enumerated from the tumors harvested from mice with or without GCV. The cell density was determined in 10 randomly chosen tumor areas at 400-fold magnification. Bars, ±1 SD; *, $P < 0.05$, compared with WT. (C) Immunohistochemical analysis was performed using anti-CD3, anti-DEC205, or anti-CD11c antibody on tumors after GCV treatment in WT and KO mice. Representative results from three individual animals in each group are shown here. Original magnification, ×400. Original bars, 50 μm.

WT mice (Fig. 5D). Increases in $CD8^+IFN\text{-}\gamma^+$ cells were less evident in CCR1KO, CCR5KO, or CCL3KO mice treated with tumor cells and GCV compared with WT mice when lymph node-derived cells were cocultured with BNL cell lysates (Fig. 5D). These observations suggest that the absence of CCR1, CCR5, or CCL3 greatly impaired the apoptosis-induced establishment of specific tumor immunity.

Apoptosis-induced migration of DCs to draining lymph nodes and intranodal T cell proliferation activation in a CCR1-, CCR5-, and/or CCL3-dependent manner

Tumor-infiltrating DCs can uptake tumor antigens at the tumor sites and migrate to the draining lymph nodes, where they mature to present antigens to T cells [17, 18]. Thus, we further explored the status of DCs as well as T cells in the draining lymph nodes. Following GCV treatment, tumor apoptosis increased the proportions of $CD86^+CD11c^+$ cells in the draining lymph nodes but not in distant lymph nodes in WT mice (**Fig. 6A**). In contrast, GCV-induced increases in $CD11c^+$ cell proportion were depressed in CCR1KO, CCR5KO, or CCL3KO mice (Fig. 6A). The levels of CD86 on $CD11c^+$ cells were increased in GCV-treated WT mice compared with WT mice, which had been injected with neither BNL-tk cells nor GCV, although the levels of CD86 were depressed in the KO mice (mean fluorescent intensities of CD86 on $CD11c^+$ cells: WT/BNL-tk/GCV, 114.3±8.6; WT/BNL-tk, 86.2±12.2; WT/no tumor, 86.5±2.6; CCR1KO/BNL-tk/GCV, 85.4±15.6; CCR5KO/BNL-tk/GCV, 92.3±12.6; CCL3KO/BNL-tk/GCV, 79.0±9.8). Moreover, GCV-induced tumor apoptosis significantly increased the numbers of total cells, $CD4^+$ and $CD8^+$ cells, in the draining lymph nodes of WT mice. GCV-induced increases in these cell populations were also attenuated in CCR1KO, CCR5KO, or CCL3KO mice (Fig. 6B). Lymphocytes expressing the cell proliferation marker Ki67 were increased in the paracortical areas of the draining lymph nodes of GCV-treated WT mice compared with the other groups (Fig. 6C and Supplemental Fig. 5). Injection of BNL-tk cells marginally increased the proportion of activated $CD4^+$ T cells, defined as $CD44^{hi}CD62L^{lo}CD4^+$, in the draining lymph nodes. Coinjec-

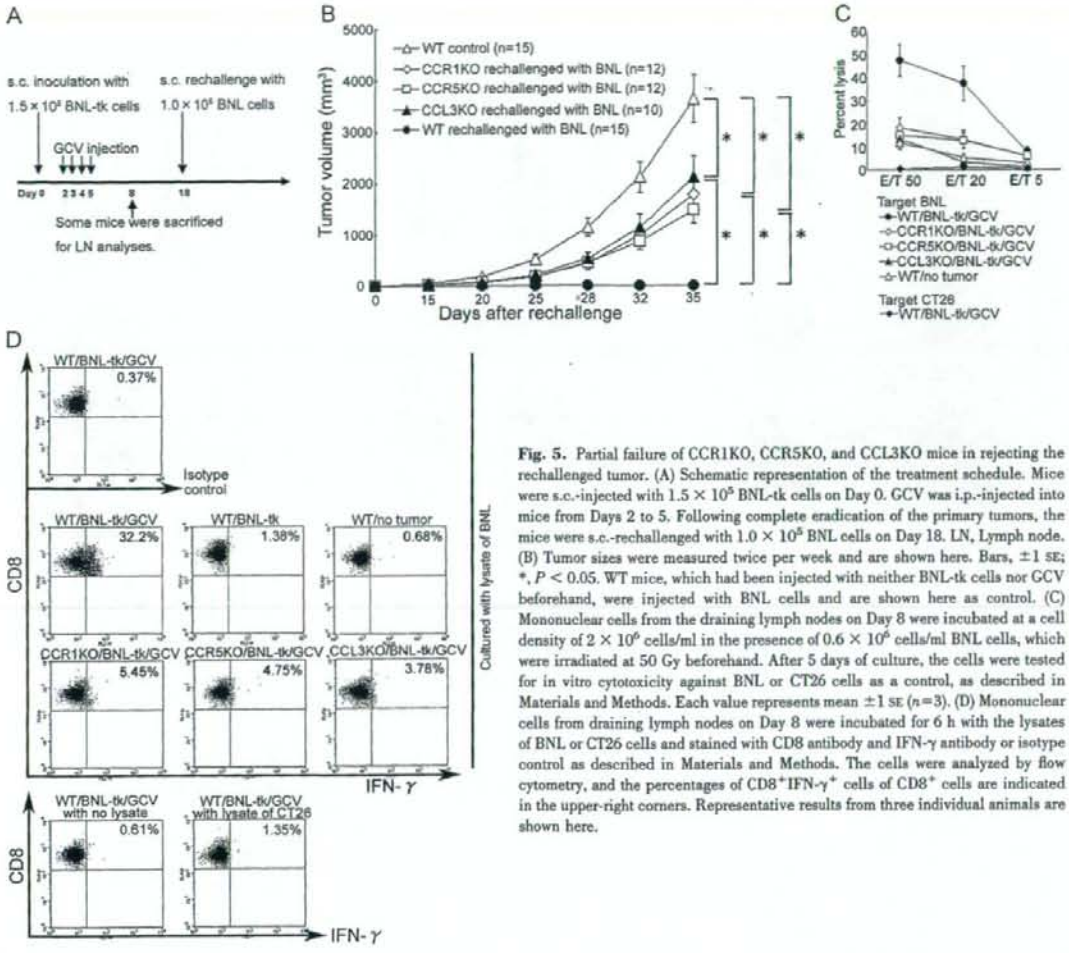

Fig. 5. Partial failure of CCR1KO, CCR5KO, and CCL3KO mice in rejecting the rechallenged tumor. (A) Schematic representation of the treatment schedule. Mice were s.c.-injected with 1.5×10^5 BNL-tk cells on Day 0. GCV was i.p.-injected into mice from Days 2 to 5. Following complete eradication of the primary tumors, the mice were s.c.-rechallenged with 1.0×10^5 BNL cells on Day 18. LN, Lymph node. (B) Tumor sizes were measured twice per week and are shown here. Bars, ±1 SE; *, $P < 0.05$. WT mice, which had been injected with neither BNL-tk cells nor GCV beforehand, were injected with BNL cells and are shown here as control. (C) Mononuclear cells from the draining lymph nodes on Day 8 were incubated at a cell density of 2×10^6 cells/ml in the presence of 0.6×10^6 cells/ml BNL cells, which were irradiated at 50 Gy beforehand. After 5 days of culture, the cells were tested for in vitro cytotoxicity against BNL or CT26 cells as a control, as described in Materials and Methods. Each value represents mean ±1 SE ($n=3$). (D) Mononuclear cells from draining lymph nodes on Day 8 were incubated for 6 h with the lysates of BNL or CT26 cells and stained with CD8 antibody and IFN-γ antibody or isotype control as described in Materials and Methods. The cells were analyzed by flow cytometry, and the percentages of $CD8^+IFN\text{-}\gamma^+$ cells of $CD8^+$ cells are indicated in the upper-right corners. Representative results from three individual animals are shown here.

tion of GCV further augmented this increment in WT mice but not in KO mice (Fig. 6, D and E). These observations suggest that the absence of CCR1, CCR5, or CCL3 impaired the GCV-induced migration of DCs into the draining lymph nodes and the subsequent proliferation and activation of T cells in the draining lymph nodes.

Restoration of anti-tumor response of KO mice by adoptive transfer of DCs harvested from GCV-treated WT mice

Given the proposed, crucial role of DCs in evoking antitumor immunity after tumor apoptosis, we finally performed adoptive transfer of DCs harvested from the draining lymph nodes of GCV-treated WT mice into the KO mice. DCs were harvested from the draining lymph nodes of GCV-treated, tumor-bearing or tumor-free WT mice and were transferred s.c. into the KO mice on Day 8 (Fig. 5A). The KO mice completely rejected the rechallenged cells when DCs were transferred from GCV-treated, tumor-bearing WT mice but not tumor-free WT mice (**Fig. 7**). These observations suggest that GCV-induced tumor apoptosis mediated the trafficking of DCs to the draining lymph nodes, which can induce the establishment of specific immunity in a CCR1-, CCR5-, or CCL3-dependent manner.

DISCUSSION

Apoptosis was previously presumed to be immunologically silent or even tolerogenic [27]. However, recent reports have indicated that tumor cell apoptosis can induce antitumor immune responses effectively, as the immunogenicity of apoptotic tumor cells is dependent on apoptosis inducers. Indeed, gemcitabine-induced apoptosis can augment cross-priming of tumor-specific $CD8^+$ T cells in vivo rather than cross-tolerizing [8]. Similarly, apoptosis induced by local radiation therapy can generate tumor antigen-specific effector cells that migrate to

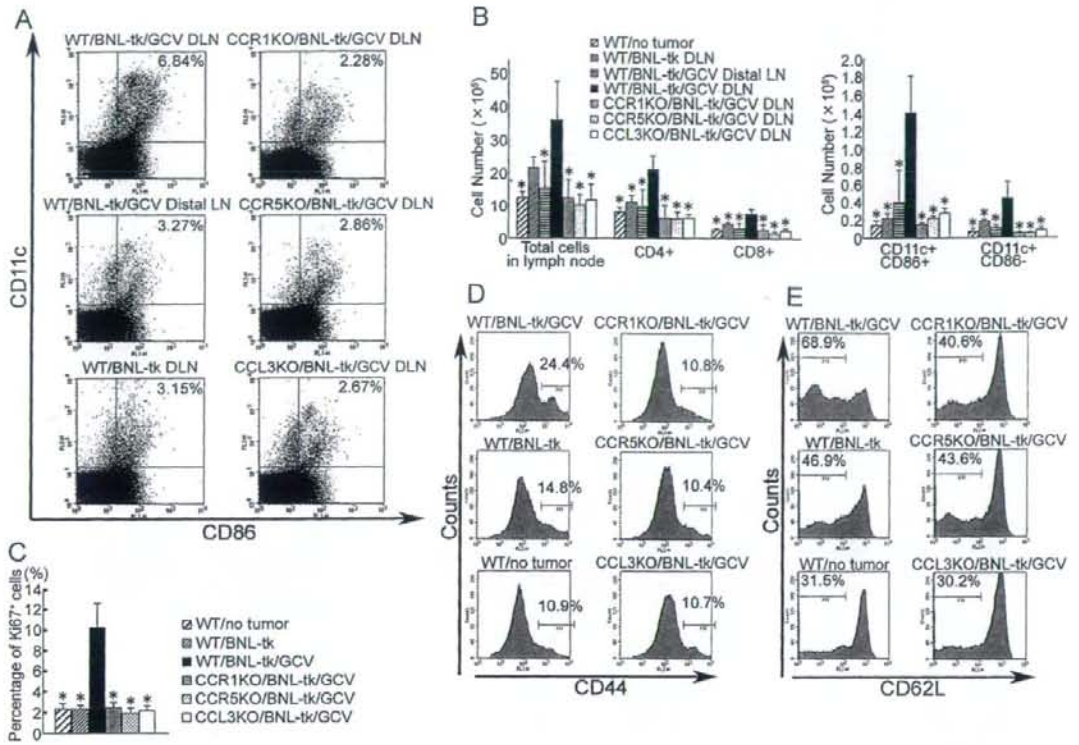

Fig. 6. Apoptosis-induced migration of DCs to the draining lymph nodes (DLN) and intranodal T cell proliferation and activation in a CCR1-, CCR5-, and/or CCL3-dependent manner. Mice were treated according to the schedule shown in Figure 5A. (A) Draining lymph nodes or distal lymph nodes were harvested on Day 8 as indicated in Figure 5A. Mononuclear cells were stained with a combination of FITC-labeled anti-CD86 and PE-labeled anti-CD11c antibodies. The percentage of $CD11c^+CD86^+$ cells was determined and is indicated in the upper-right corners. Representative results from three individual animals are shown here. (B) Absolute cell numbers of each cell population in the draining lymph nodes or distal lymph nodes on Day 8 were determined as described in Materials and Methods. Error bars, ±1 SD; *, $P < 0.05$, compared with draining lymph nodes derived from WT mice treated with BNL-tk/GCV. (C) Draining lymph nodes harvested on Day 8 were immunostained with anti-Ki67 antibody, and percentages of $Ki67^+$ cells in lymph nodes were determined. Error bars, ±1 SD; *, $P < 0.05$, compared with draining lymph nodes derived from WT mice treated with BNL-tk/GCV. (D and E) Mononuclear cells harvested on Day 8 were stained with a combination of FITC-labeled anti-CD4 and PE-labeled anti-CD44 (D) or PE-labeled anti-CD62L (E) antibodies. Histograms were gated on CD4-positive cells, and percentages of $CD44^{hi}$ (D) or $CD62L^{lo}$ (E) cells were determined. Representative results from three individual animals are shown here.

the tumor [28]. Moreover, apoptotic change caused by anthracyclin can induce the translocation of calreticulin to the apoptotic tumor cell surface, and calreticulin exposure can enhance the immunogenicity of apoptotic cancer cells [6, 7]. Thus, apoptosis induced by these measures is sufficiently immunogenic to prevent tumor progression.

The combination of HSV-tk gene transfer and GCV can efficiently induce the apoptosis of the transfected tumors as observed in the present study. Here, we also observed that the treatment augmented the immune response, as evidenced by an increase in the number of tumor-infiltrating DCs. Subsequently, the number of DCs in the draining lymph nodes increased together with enhanced, specific immunity to the injected tumor. These observations suggest that tumor apoptosis induced by HSV-tk/GCV treatment is effective in generating specific tumor immunity, similar to that observed in the case of anticancer drug treatment.

Consistent with our present observations, CCL3 and its related chemokine CCL5 were detected in macrophages infiltrating human cancer tissues [29, 30]. Given their potent chemotactic activity against various types of immune cells [31], gene transfer of CCL3 or CCL5 induced the accumulation of immune cells including DCs, T cells, macrophages, and NK cells in the tumor sites, resulting in delayed tumor growth and prolonged survival [16, 32–34]. Moreover, combination therapy of the HSV-tk and CCL3/CCL20 gene induces an exaggerated accumulation of DCs, $CD4^+$ cells, $CD8^+$ cells, NK cells, and macrophages in the tumor sites compared with HSV-tk/GCV treatment alone, and the net effects are tumor regression and prolonged survival [34]. However, the roles of endogenously produced CCL3 and its related chemokines in tumor apoptosis still remain to be elucidated.

In human HCC, tumor-infiltrating lymphocytes express high levels of CCR5 and CXCR3. Moreover, these lymphocytes

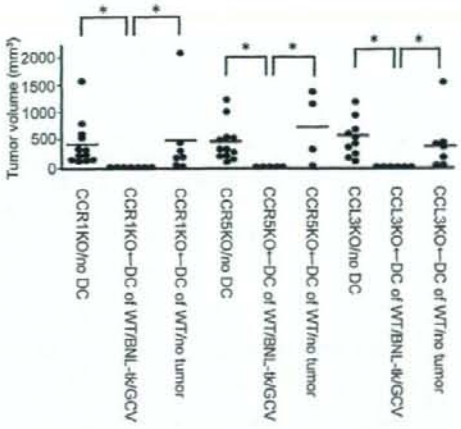

Fig. 7. Adoptive transfer of DCs harvested from GCV-treated WT mice restored the antitumor response of KO mice. After inoculation of BNL-tk tumors, CCR1KO, CCR5KO, or CCL3KO mice were treated with GCV from Days 2 to 5 as described in Figure 5A. The DCs were then harvested from the draining lymph nodes of GCV-treated WT mice and transferred s.c. into the KO mice on Day 8 as shown in Figure 5A. On Day 18, these mice were injected again with parental BNL cells, and tumor sizes were measured on Day 28. GCV-treated KO mice, transferred without or with DCs of naïve WT mice, were also rechallenged with parental BNL cells as control. Bars, mean; *, $P < 0.05$.

show strong chemotactic responses to CC and CXC chemokines including CCL3, CCL4, and CXCL9 [35]. Additional treatments are nevertheless required to enhance the immune responses, as the CCR5- or CXCR3-positive lymphocytes are insufficient to evoke immune responses and eradicate tumor tissues. We demonstrated that suicide gene therapy-induced tumor cell apoptosis augments CCR1- and CCR5-positive cell infiltration into the hepatoma tissues. Further, these CCR1- or CCR5-positive cells are DCs and/or T cells—the cells indispensable for tumor immunity. Thus, suicide gene therapy can potentially enhance tumor immunity by attracting these immune cells to the apoptotic tumor cells.

The initial step leading to specific tumor immunity is the capture of tumor antigens by macrophages and immature DCs, both of which accumulate in tumor sites. However, in this model, CCR1KO, CCR5KO, and CCL3KO mice failed to completely eliminate the rechallenged tumor cells along with reduced intratumoral accumulation of DCs but not F4/80-positive macrophages. These observations suggest that the establishment of specific tumor immunity requires intratumoral recruitment of immature DCs but not macrophages. Activated NK cells can also induce DC maturation in lymphoid organs as well as in nonlymphoid tissues. Although NK cells express chemokine receptors such as CCR5 [36], the deficiency of CCR1 or CCR5 has little effects on intratumoral infiltration of NK cells. These observations preclude the crucial role of NK cells in the establishment of specific tumor immunity in this model.

Immature DCs use several chemokine receptors including CCR1, CCR2, CCR4, CCR5, CCR6, CCR8, and CXCR4 for their migration [22]. However, the chemokine receptor(s) regulating immature DC trafficking to tumor sites still need(s) to be determined. We previously observed that CCL3 induced mobilization of DC precursors into circulation [37] and detected CCL3 in tumor-infiltrating $CD3^+$ T cells and macrophages after GCV treatment. Therefore, we investigated the roles of CCL3 and its receptors CCR1 and CCR5 in the intratumoral recruitment of DCs and the subsequent establishment of specific tumor immunity. Although CCL4 and CCL5 expression was augmented along with CCL3 expression in tumor sites, the deletion of the *CCL3* gene alone markedly reduced the DC migration, intranodal T cell accumulation, and subsequent Th1 cytokine expression. Similarly, deletion of the *CCL3* gene alone prevented coxsackievirus-induced myocarditis [38], despite enhanced, intracardiac expression of CCL3, CCL4, and CCL5 mRNA [39]. Thus, these three chemokines may form a positive feedback loop, and the deletion of either chemokine might reduce the expression of the others. Moreover, the lack of CCR1 or CCR5 reduces the migration of DCs to tumor sites and subsequent tumor immunity in the draining lymph nodes, such as DC and T cell accumulation and Th1 cytokine expression. As almost all CD11c- and DEC205-positive DCs express CCR1 and CCR5, DC migration may require coordinated and synergistic actions of both of these chemokine receptors.

We have provided definitive evidence regarding the essential contribution of CCL3 and its receptors to apoptosis-induced, specific tumor immunity, which exert their role by attracting DCs to tumor tissues. These observations further suggest that specific tumor immunity can be established more efficiently if some techniques such as chemokine gene transfer can augment the recruitment of immature DCs to apoptotic tumor tissues caused by chemotherapeutic agents and/or irradiation as well as suicide gene therapy.

ACKNOWLEDGMENTS

We thank Dr. Philip M. Murphy (NIAID, NIH) for providing us with CCR1KO mice. We also thank Dr. Toshikazu Kondo (Wakayama Medical University, Wakayama, Japan) for his technical advice about double-color immunofluorescence analysis.

REFERENCES

1. Tsukuma, H., Hiyama, T., Tanaka, S., Nakao, M., Yabuuchi, T., Kitamura, T., Nakanishi, K., Fujimoto, I., Inoue, A., Yamazaki, H., Kawashima, T. (1993) Risk factors for hepatocellular carcinoma among patients with chronic liver disease. *N. Engl. J. Med.* **328,** 1797–1801.
2. Velázquez, R. F., Rodríguez, M., Navascués, C. A., Linares, A., Pérez, R., Sotorríos, N. G., Martínez, I., Rodrigo, L. (2003) Prospective analysis of risk factors for hepatocellular carcinoma in patients with liver cirrhosis. *Hepatology.* **37,** 520–527.
3. Okita, K. (2006) Management of hepatocellular carcinoma in Japan. *J. Gastroenterol.* **41,** 100–106.
4. Poon, R. T., Fan, S. T., Ng, I. O., Lo, C. M., Liu, C. L., Wong, J. (2000) Different risk factors and prognosis for early and late intrahepatic recurrence after resection of hepatocellular carcinoma. *Cancer* **89,** 500–507.
5. Butterfield, L. H. (2004) Immunotherapeutic strategy for hepatocellular carcinoma. *Gastroenterology* **127,** S232–S241.
6. Obeid, M., Tesniere, A., Ghiringhelli, F., Fimia, G. M., Apetoh, L., Perfettini, J. L., Castedo, M., Mignot, G., Panaretakis, T., Casares, N.,

Métivier, D., Larochette, N., van Endert, P., Ciccosanti, F., Piacentini, M., Zitvogel, L., Kroemer, G. (2007) Calreticulin exposure dictates the immunogenicity of cancer cell death. *Nat. Med.* **13,** 54–61.
7. Casares, N., Pequignot, M. O., Tesniere, A., Ghiringhelli, F., Roux, S., Chaput, N., Schmitt, E., Hamai, A., Hervas-Stubbs, S., Obeid, M., Coutant, F., Métivier, D., Pichard, E., Aucouturier, P., Pierron, G., Garrido, C., Zitvogel, L., Kroemer, G. (2005) Caspase-dependent immunogenicity of doxorubicin-induced tumor cell death. *J. Exp. Med.* **202,** 1691–1701.
8. Nowak, A. K., Lake, R. A., Marzo, A. L., Scott, B., Heath, W. R., Collins, E. J., Frelinger, J. A., Robinson, B. W. S. (2003) Induction of tumor cell apoptosis in vivo increases tumor antigen cross-presentation, cross-priming rather than cross-tolerizing host tumor-specific CD8 T cells. *J. Immunol.* **170,** 4905–4913.
9. Hamel, W., Magnelli, L., Chiarugi, V. P., Israel, M. A. (1996) Herpes simplex virus thymidine kinase/ganciclovir-mediated apoptotic death of bystander cells. *Cancer Res.* **56,** 2697–2702.
10. Beltinger, C., Fulda, S., Kammertoens, T., Meyer, E., Uckert, W., Debatin, K. M. (1999) Herpes simplex virus thymidine kinase/ganciclovir-induced apoptosis involves ligand-independent death receptor aggregation and activation of caspases. *Proc. Natl. Acad. Sci. USA* **96,** 8699–8704.
11. Freeman, S. M., Ramesh, R., Marrogi, A. J. (1997) Immune system in suicide-gene therapy. *Lancet* **349,** 2–3.
12. Vile, R. G., Castleden, S., Marshall, J., Camplejohn, R., Upton, C., Chong, H. (1997) Generation of an anti-tumor immune response in a non-immunogenic tumor: HSVtk killing in vivo stimulates a mononuclear cell infiltrate and a Th1-like profile of intratumoural cytokine expression. *Int. J. Cancer* **71,** 267–274.
13. Freeman, S. M., Ramesh, R., Shastri, M., Munshi, A., Jensen, A. K., Marrogi, A. J. (1995) The role of cytokines in mediating the bystander effect using HSV-TK xenogeneic cells. *Cancer Lett.* **92,** 167–174.
14. Chen, S. H., Chen, X. H. L., Wang, Y., Kosai, K., Finegold, M. J., Rich, S. S., Woo, S. L. C. (1995) Combination gene therapy for liver metastasis of colon carcinoma in vivo. *Proc. Natl. Acad. Sci. USA* **92,** 2577–2581.
15. Chen, S. H., Kosai, K., Xu, B., Pham-Nguyen, K., Contant, C., Finegold, M. J., Woo, S. L. C. (1996) Combination suicide and cytokine gene therapy for hepatic metastases of colon carcinoma: sustained antitumor immunity prolongs animal survival. *Cancer Res.* **56,** 3758–3762.
16. Tsuchiyama, T., Nakamoto, Y., Sakai, Y., Marukawa, Y., Kitahara, M., Mukaida, N., Kaneko, S. (2007) Prolonged, NK cell-mediated antitumor effects of suicide gene therapy combined with monocyte chemoattractant protein-1 against hepatocellular carcinoma. *J. Immunol.* **178,** 574–583.
17. Banchereau, J., Steinman, R. M. (1998) Dendritic cells and the control of immunity. *Nature* **392,** 245–252.
18. Sallusto, F., Lanzavecchia, A. (1999) Mobilizing dendritic cells for tolerance, priming, and chronic inflammation. *J. Exp. Med.* **189,** 611–614.
19. Castellino, F., Huang, A. Y., Altan-Bonnet, G., Stoll, S., Scheinecker, C., Germain, R. N. (2006) Chemokines enhance immunity by guiding naïve $CD8^+$ T cells to sites of $CD4^+$ T cell-dendritic cell interaction. *Nature* **440,** 890–895.
20. Dieu, M. C., Vanbervliet, B., Vicari, A., Bridon, J. M., Oldham, E., Ait-Yahia, S., Brière, F., Zlotnik, A., Lebecque, S., Caux, C. (1998) Selective recruitment of immature and mature dendritic cells by distinct chemokines expressed in different anatomic sites. *J. Exp. Med.* **188,** 373–386.
21. Sozzani, S., Luini, W., Borsatti, A., Polentarutti, N., Zhou, D., Piemonti, L., D'Amico, G., Power, C. A., Wells, T. N. C., Gobbi, M., Allavena, P., Mantovani, A. (1997) Receptor expression and responsiveness of human dendritic cells to a defined set of CC and CXC chemokines. *J. Immunol.* **159,** 1993–2000.
22. Sozzani, S. (2005) Dendritic cell trafficking: more than just chemokines. *Cytokine Growth Factor Rev.* **16,** 581–592.
23. Murai, M., Yoneyama, H., Ezaki, T., Suematsu, M., Terashima, Y., Harada, A., Hamada, H., Asakura, H., Ishikawa, H., Matsushima, K. (2003) Peyer's patch is the essential site in initiating murine acute and lethal graft-versus-host reaction. *Nat. Immunol.* **4,** 154–160.
24. Tsuchiyama, T., Kaneko, S., Nakamoto, Y., Sakai, Y., Honda, M., Mukaida, N., Kobayashi, K. (2003) Enhanced antitumor effects of a bicistronic adenovirus vector expressing both herpes simplex virus thymidine kinase and monocyte chemoattractant protein-1 against hepatocellular carcinoma. *Cancer Gene Ther.* **10,** 260–269.
25. Murai, M., Yoneyama, H., Harada, A., Yi, Z., Vestergaard, C., Guo, B., Suzuki, K., Asakura, H., Matsushima, K. (1999) Active participation of $CCR5^+CD8^+$ T lymphocytes in the pathogenesis of liver injury in graft-versus-host disease. *J. Clin. Invest.* **104,** 49–57.
26. Lu, P., Nakamoto, Y., Nemoto-Sakai, Y., Fujii, C., Wang, H., Hashii, M., Ohmoto, Y., Kaneko, S., Kobayashi, K., Mukaida, N. (2003) Potential interaction between CCR1 and its ligand, CCL3, induced by endogeneously produced interleukin-1 in human hepatomas. *Am. J. Pathol.* **162,** 1249–1258.
27. Steinman, R. M., Turley, S., Mellman, I., Inaba, K. (2000) The induction of tolerance by dendritic cells that have captured apoptotic cells. *J. Exp. Med.* **191,** 411–416.
28. Lugade, A. A., Moran, J. P., Gerber, S. A., Rose, R. C., Frelinger, J. G., Lord, E. M. (2005) Local radiation therapy of B16 melanoma tumors increases the generation of tumor antigen-specific effector cells that traffic to the tumor. *J. Immunol.* **174,** 7516–7523.
29. Tang, K. F., Tan, S. Y., Chan, S. H., Chong, S. M., Loh, K. S., Tan, L. K. S., Hu, H. (2001) A distinct expression of CC chemokines by macrophages in nasopharyngeal carcinoma: implication for the intense tumor infiltration by T lymphocytes and macrophages. *Hum. Pathol.* **32,** 42–49.
30. Musha, H., Ohtani, H., Mizoi, T., Kinouchi, M., Nakayama, T., Shiiba, K., Miyagawa, K., Nagura, H., Yoshie, O., Sasaki, I. (2005) Selective infiltration of $CCR5^+CXCR3^+$ T lymphocytes in human colorectal carcinoma. *Int. J. Cancer* **116,** 949–956.
31. Menten, P., Wuyts, A., van Damme, J. (2002) Macrophage inflammatory protein-1. *Cytokine Growth Factor Rev.* **13,** 455–481.
32. Lavergne, E., Combadière, C., Iga, M., Boissonnas, A., Bonduelle, O., Maho, M., Debré, P., Combadiere, B. (2004) Intratumoral CC chemokine ligand 5 overexpression delays tumor growth and increases tumor cell infiltration. *J. Immunol.* **173,** 3755–3762.
33. Fushimi, T., Kojima, A., Moore, M. A., Crystal, R. G. (2000) Macrophage inflammatory protein 3α transgene attracts dendritic cells to established murine tumors and suppresses tumor growth. *J. Clin. Invest.* **105,** 1383–1393.
34. Crittenden, M., Gough, M., Harrington, K., Olivier, K., Thompson, J., Vile, R. G. (2003) Expression of inflammatory chemokines combined with local tumor destruction enhances tumor regression and long-term immunity. *Cancer Res.* **63,** 5505–5512.
35. Yoong, K. F., Afford, S. C., Jones, R., Aujla, P., Qin, S., Price, K., Hubscher, S. G., Adams, D. H. (1999) Expression of CXC and CC chemokines in human malignant liver tumors: a role for human monokine induced by γ-interferon in lymphocyte recruitment to hepatocellular carcinoma. *Hepatology* **30,** 100–111.
36. Walzer, T., Dalod, M., Robbins, S. H., Zitvogel, L., Vivier, E. (2005) Natural-killer cells and dendritic cells: "l'union fait la force". *Blood* **106,** 2252–2258.
37. Zhang, Y., Yoneyama, H., Wang, Y., Ishikawa, S., Hashimoto, S., Gao, J. L., Murphy, P. M., Matsushima, K. (2004) Mobilization of dendritic cell precursors into the circulation by administration of MIP-1α in mice. *J. Natl. Cancer Inst.* **96,** 201–209.
38. Cook, D. N., Beck, M. A., Coffman, T. M., Kirby, S. L., Sheridan, J. F., Pragnell, I. B., Smithies, O. (1995) Requirement for an inflammatory response to viral infection. *Science* **269,** 1583–1585.
39. Gebhard, J. R., Perry, C. M., Harkins, S., Lane, T., Mena, I., Asensio, V. C., Campbell, I. L., Whitton, J. L. (1998) Coxsackievirus B3-induced myocarditis. Perforin exacerbates disease, but plays no detectable role in virus clearance. *Am. J. Pathol.* **153,** 417–428.

ELSEVIER

Journal of Hepatology 49 (2008) 946–954

Journal of Hepatology

www.elsevier.com/locate/jhep

Expression of multidrug resistance-associated protein 3 and cytotoxic T cell responses in patients with hepatocellular carcinoma☆

Eishiro Mizukoshi, Masao Honda, Kuniaki Arai, Tatsuya Yamashita, Yasunari Nakamoto, Shuichi Kaneko*

Department of Gastroenterology, Graduate School of Medicine, Kanazawa University, Kanazawa, Ishikawa 920-8641, Japan

***Background/Aims*: Multidrug resistance-associated protein 3 (MRP3) is a carrier-type transport protein belonging to the ABC transporters. It is expressed in normal tissues, and enhanced expression in many cancers has been reported. In this study, we investigated the usefulness of MRP3 as a target antigen in immunotherapy for hepatocellular carcinoma (HCC).**

***Methods*: The MRP3 expression level in HCC tissue was measured by quantitative PCR. MRP3-specific T cell responses were investigated by several immunological techniques using peripheral blood mononuclear cells or tumor-infiltrating lymphocytes.**

***Results*: The MRP3 expression level in HCC tissue was significantly higher than that in non-cancerous tissue ($P < 0.05$). MRP3-specific cytotoxic T cells (CTLs) could be induced regardless of liver function, the presence or absence of HCV infection, the blood AFP level, and the stage of HCC. The CTLs showed cytotoxicity against HCC cells overexpressing MRP3. A negative correlation was present between the MRP3 expression level in HCC tissue and the frequency of MRP3-specific CTLs. The frequency of MRP3-specific CTLs increased after HCC treatment, such as transcatheter arterial embolization and radiofrequency ablation.**

***Conclusions*: Our study demonstrates that MRP3 is a potential candidate for tumor antigen with strong immunogenicity in HCC immunotherapy.**

***Keywords*: Immune response; CD8; HLA-A24; Hepatitis; Cancer**

1. Introduction

Hepatocellular carcinoma (HCC) is treatable by hepatectomy or percutaneous ablation when the lesion is localized to some extent, and radical therapeutic effects can be obtained when the resection or cauterization with a safety margin can be performed [1,2]. However, active hepatitis and cirrhosis in the surrounding non-tumor liver tissues exhibit high carcinogenetic potentials to develop *de novo* HCC, and therefore, the recurrence rate of HCC after treatment is very high [3,4].

To protect against recurrence, tumor antigen-specific immunotherapy is an attractive strategy. For the development of HCC-specific immunotherapy and analysis of immune responses to the treatment, the identification of HCC-specific tumor antigens or their antigenic epitopes is necessary. However, only a few HCC-specific tumor antigens and their antigenic epitopes have been identified [5–10].

MRP3 is a carrier-type transport protein belonging to the ABC transporters that transport substances against

Received 11 January 2008; received in revised form 23 April 2008; accepted 7 May 2008; available online 5 June 2008

Associate Editor: V. Barnaba

☆ The authors declare that they do not have anything to disclose regarding funding from industries or conflict of interest with respect to this manuscript.

* Corresponding author. Tel.. +81 76 265 2230; fax: +81 76 234 4250.

E-mail address: skaneko@m-kanazawa.jp (S. Kaneko).

Abbreviations: HLA, human leukocyte antigen; IFN, interferon; PBMC, peripheral blood mononuclear cell; TIL, tumor-infiltrating lymphocytes; HCV, hepatitis C virus; ELISPOT, enzyme linked immunospot.

0168-8278/$34.00 © 2008 European Association for the Study of the Liver. Published by Elsevier B.V. All rights reserved.
doi:10.1016/j.jhep.2008.05.012

the concentration gradient in an ATP energy-dependent manner [11]. It is expressed at a high level in the small and large intestine, pancreas, placenta, and adrenal cortex [12], and recent studies have reported that its expression is enhanced in various cancer cells [13–15]. Yamada et al. demonstrated that MRP3 was a tumor rejection antigen recognized by cytotoxic T cells (CTLs), using lymphocytes infiltrating into lung adenocarcinoma, and identified its CTL epitope [13]. These reports suggest that MRP3 may be useful as a target antigen in HCC immunotherapy. However, the MRP3 expression level in HCC tissue has been controversial [16,17], and the association between the expression level and the degree of the immune response to MRP3 in HCC patients has not been clarified.

In this study, we measured the MRP3 expression level in various hematoma cell lines and HCC tissues in HCC patients, and analyzed immune responses to MRP3 using peripheral blood mononuclear cells (PBMCs) and tumor-infiltrating lymphocytes (TILs) to investigate the usefulness of MRP3 in HCC immunotherapy.

2. Materials and methods

2.1. Patients

This study examined 103 HLA-A24-positive patients with HCC (Table 1). All subjects were negative for Abs to human immunodeficiency virus (HIV), and gave written informed consent to participate in this study in accordance with the Helsinki declaration. The diagnosis of HCC was histologically confirmed by taking US-guided needle biopsy specimens in 35 cases, surgical resection in 13 cases, and autopsy in 4 cases. For the remaining 51 patients, the diagnosis was based on typical hypervascular tumor staining on angiography in addition to typical findings, which showed hyperattenuated areas in the early phase and hypoattenuation in the late phase on dynamic CT [18]. Eleven healthy blood donors with HLA-A24, who did not have a history of cancer and were negative for HBsAg and anti-HCVAb, served as controls.

2.2. Laboratory and virologic testing

Blood samples were tested for HBsAg and HCVAb by commercial immunoassays (Fuji Rebio, Tokyo, Japan). HLA-based typing of PBMC from patients and normal donors was performed as previously described [10].

The serum AFP level was measured by enzyme immunoassay (AxSYM AFP, Abbott Japan, Tokyo, Japan) and the pathological grading of tumor cell differentiation was assessed according to the general rules for the clinical and pathologic study of primary liver cancer [19]. The severity of liver disease (stage of fibrosis) was evaluated according to the criteria of Desmet et al. [20] using biopsy specimens of liver tissue, where F4 was defined as cirrhosis.

2.3. Cell lines

Eight human hepatoma cell lines: HepG2, Alex, Huh6, HLE, HLF, Hep3B, SKHep1, and Huh7, were cultured in DMEM (Gibco, Grand Island, NY, USA) with 10% fetal calf serum (FCS) (Gibco, Grand Island, NY, USA). The HLA-A*2402 gene-transfected C1R cell line (C1R-A24) [21] was cultured in RPMI 1640 medium containing 10% FCS and 500 μg/ml of hygromycin B (Sigma, St. Louis, MO, USA), and K562 was cultured in RPMI 1640 medium containing 10% FCS.

2.4. Quantitative real time detection (RTD)-PCR

We performed quantitative RTD-PCR using TaqMan Universal Master Mix (PE Applied Biosystems, Foster City, CA, USA). Primer pairs and probes for MRP3 and β-actin were obtained from TaqMan assay reagents library. Total RNA was isolated from cell lines and liver tissue samples using an RNA extraction kit (Micro RNA Extraction Kit, Stratagene, La Jolla, CA, USA). We reverse-transcribed 1 μg of isolated RNA to cDNA using SuperScript® II RT (Invitrogen, Carlsbad, CA, USA) according to the manufacturer's instructions, and the resultant cDNA was amplified with appropriate TaqMan assay reagents as previously described [22].

2.5. Preparation of PBMCs and TILs

PBMCs and TILs were isolated as previously described [9]. Fresh PBMCs were used for the CTL induction, and the remaining PBMCs and TILs were resuspended in RPMI 1640 medium containing 80% FCS and 10% dimethyl sulfoxide and cryopreserved until used. In patients with treatment, PBMCs were obtained before and 2–4 weeks after the treatment.

2.6. CTL induction and cytotoxicity assay

Peptides $MRP3_{503}$, $MRP3_{692}$, and $MRP3_{765}$, which were identified to contain a HLA-A24 restricted CTL epitope [13], were used for the induction of MRP3-specific T cells (Table 2). Peptides were synthesized at Mimotope (Melbourne, Australia) and Sumitomo Pharmaceuticals (Osaka, Japan). They were identified using mass spectrometry, and their purities were determined to be >80% by analytical HPLC. CTLs were expanded from PBMCs as previously described [23]. Briefly, four hundred thousand cells per well were stimulated with synthetic peptides at 10 μg/ml, 10 ng/ml rIL-7 and 100 pg/ml rIL-12 (Sigma, St. Louis, Mo) in RPMI 1640 supplemented with 10% heat inactivated human AB serum, 100 U/ml penicillin and 100 μg/ml streptomycin. The cultures were re-stimulated with 10 μg/ml peptide, 20 U/ml rIL-2 (Sigma, St. Louis, MO) and 10^5 mytomicin C treated autologous PBMCs on days 7 and 14. On days 3, 10 and 17, 100 μl of RPMI with 10% human AB serum and 10 U/ml rIL-2 (final concentration) was added to each well.

C1R-A24 cells and human hepatoma cell lines were used as target cells. Cytotoxicity assays were performed in at least 10 HCC patients for each peptide as previously described [10]. Spontaneous release

Table 1
Characteristics of the patients studied

Clinical diagnosis	No. of patients	Sex M/F	Age (yr) Mean ± SD	ALT (IU/L) Mean ± SD	AFP (ng/ml) mean ± SD	Etiology (B/C/B + C/Others)	Child Pugh (A/B/C)	Diff. degree[a] (Wel/Mod/Por/ND)	Tumor size[b] (Large/Small)	Tumor multiplicity (Multiple/Solitary)	Vascular Invasion (+/−)	TNM stage (I/II/IIIA/IIIB/IIIC/IV)
HCC patients	103	79/24	63 ± 10	65 ± 37	3155 ± 15946	19/73/2/9	61/39/3	17/31/4/51	79/24	73/30	30/73	24/51/16/1/3/8
Normal donors	11	8/3	35 ± 2	ND	ND	ND	ND	ND	ND	ND	ND	ND

[a] Histological degree of HCC; wel: well-differentiated, mod: moderately differentiated, por: poorly differentiated, ND: not determined.
[b] Tumor size was divided into either 'small' (≤2 cm) or 'large' (>2 cm).